原子力显微镜及其应用（2）

吴克辉

中科院物理所

致谢：王立莉

AFM Working Modes

（1）Contact mode:

（2）Tapping mode:

（3）non-contact mode

Dynamic mode

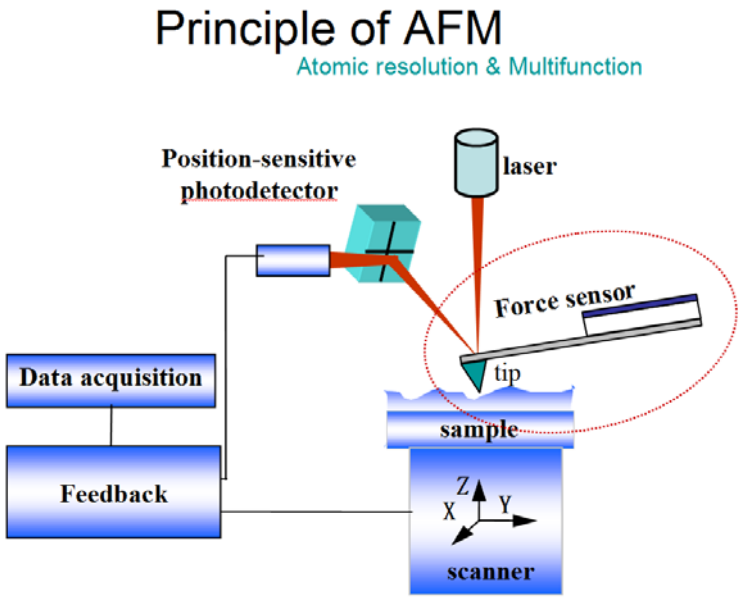

Simple model for NC-AFM

AM模式下悬梁臂受力后
振幅改变和频率改变的关系

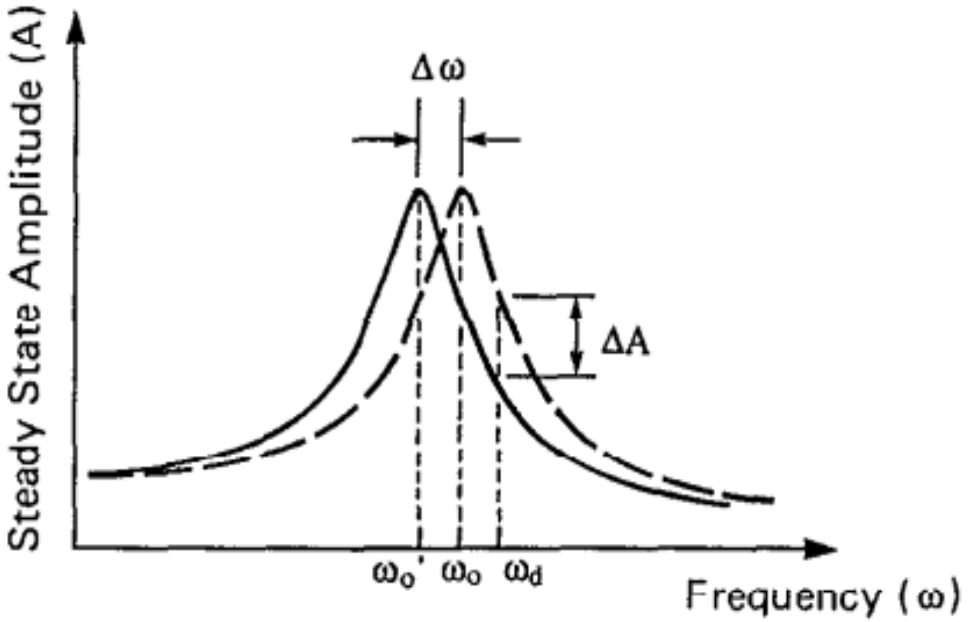

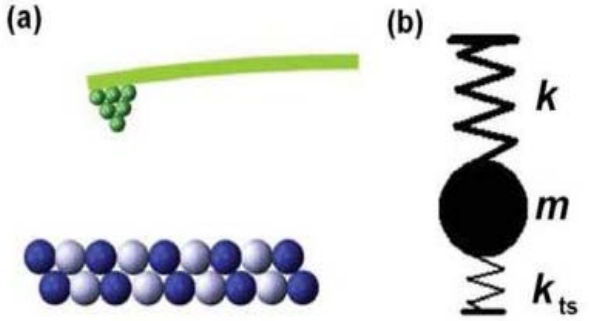

$$f = \sqrt{\frac{k + k_{ts}}{m}}$$

$$\Delta f = \frac{f_0}{2k} k_{ts}$$

Non-contact AFM

Dynamic mode

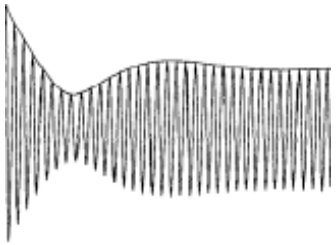

AM-AFM

Tapping mode

Image signal: amplitude

Bandwidth: $f_0/2Q$

高信噪比，高Q，慢响应，热漂移

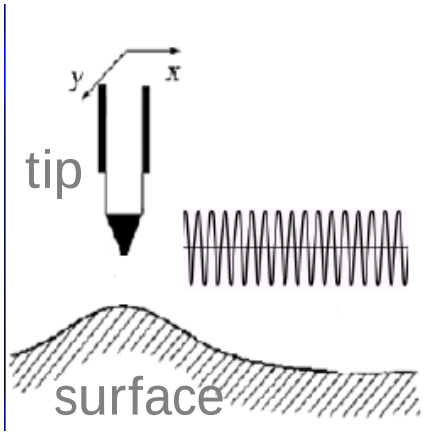

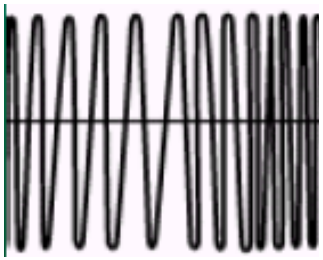

FM-AFM

Image signal: frequency shift

Bandwidth: independent of Q ➔ Fast scan

FM & AM

The role of Q-factor:
proportional to the sensitivity of image signal,
inversely proportional to thermal noise.

Block diagram of FM-AFM control system.

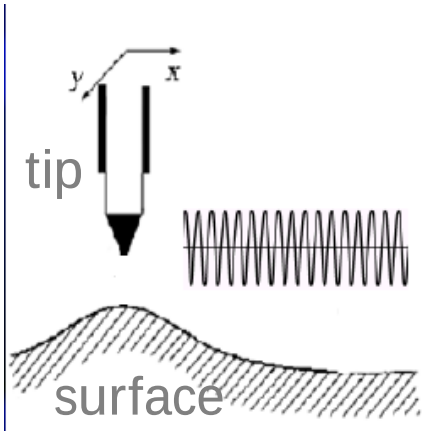

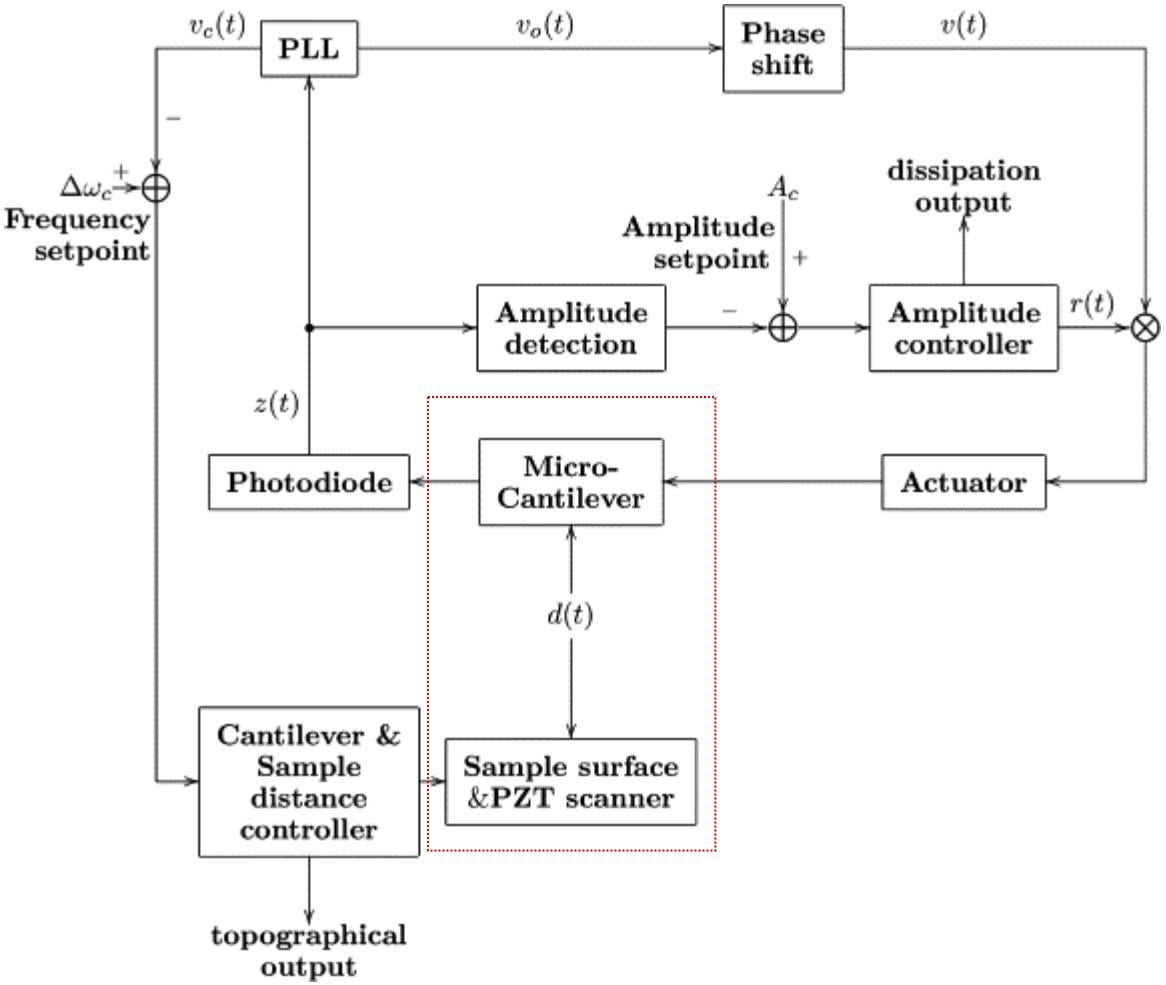

Chemical forces

$$F_{Morse} = E_{bond}/z \bullet (2e^{-\kappa(z-\sigma)} - e^{-2\kappa(z-\sigma)})$$

E_{bond} …Bond energy

κ …decay length radius

σ…equilibrium distance

Other popular choice:
12-6 Lennard Jones potential

Si(111) 7x7

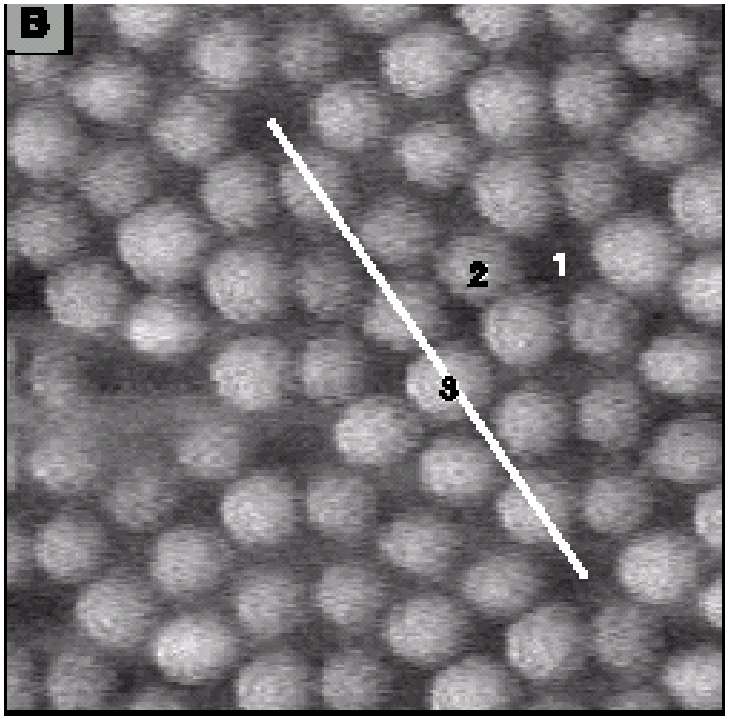

Lantz et al, Science **291**, 2580 (2001)

Other forces: electrostatic force, magnetic force, van der waals force…

Application of AFM

Application of AFM--Biology

AFM of biological samples

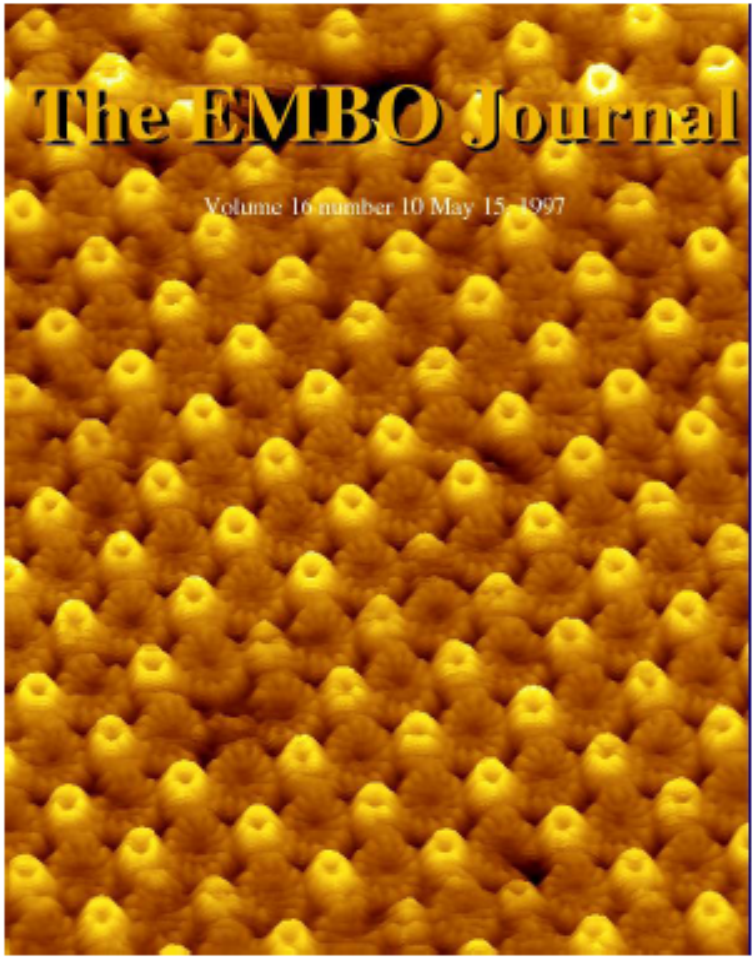

Müller et al., The bacteriophage 29 head-tail connector imaged at high resolution with the atomic force microscope in buffer solution. EMBO J. 16:2547-2553, 1997

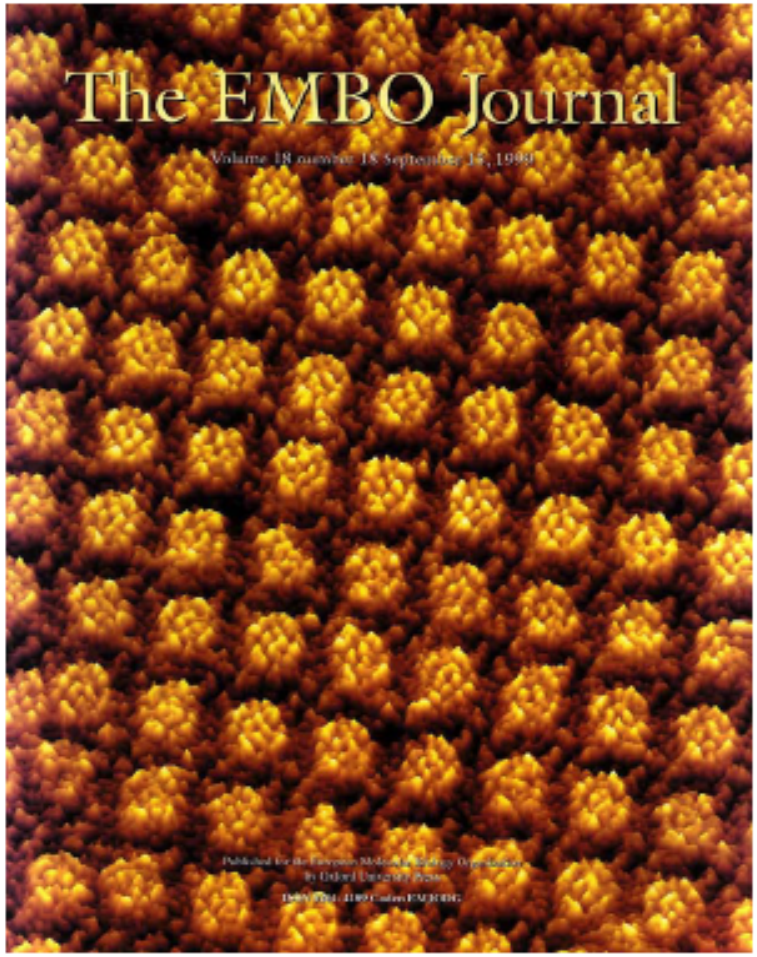

Scheuring et al., High resolution AFM topographs of the *Escherichia coli* water channel aquaporin Z. EMBO J. 18:4981-4987, 1999

Application of AFM--Biology

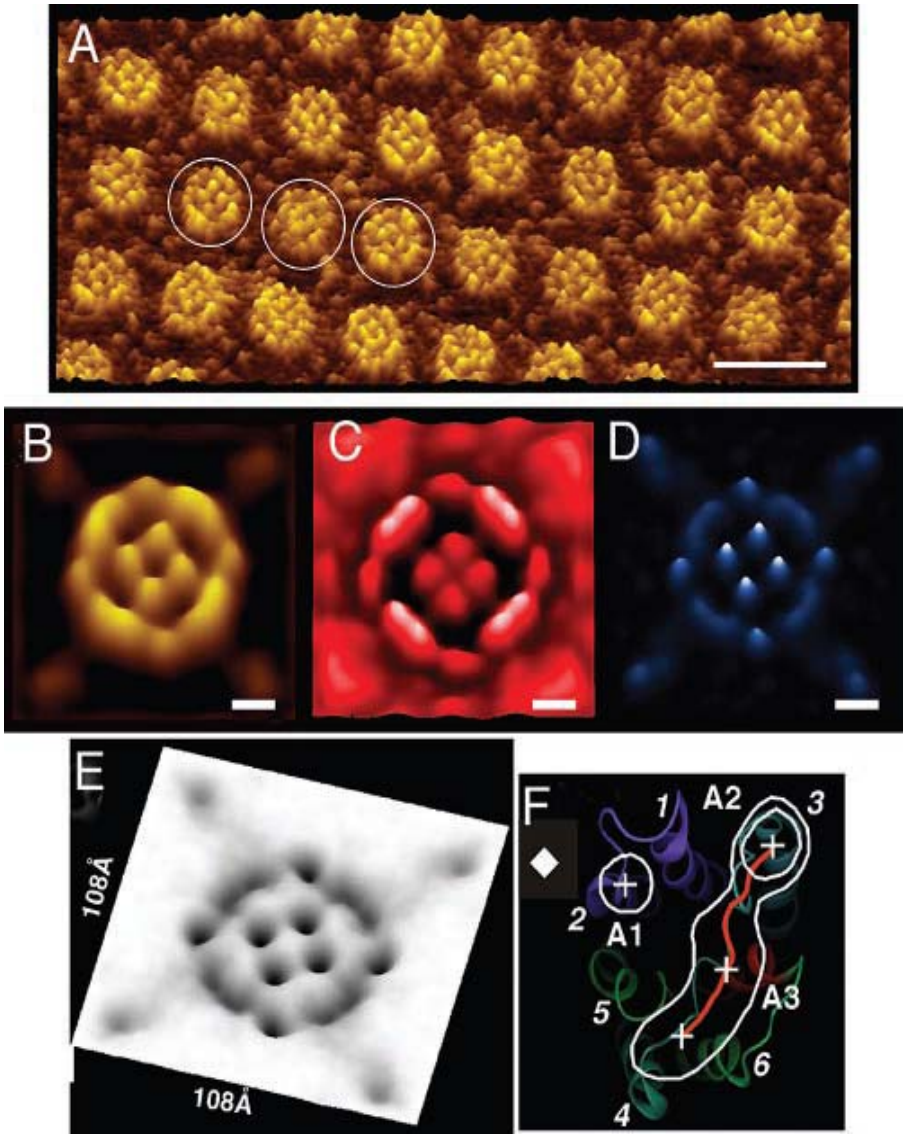

AFM image of aquaporin-Z 2D crystal

Science 302,1002(2003

Application of AFM--Biology

图3 细胞膜蛋白的结晶形态

Application of AFM--Biology

单分子力谱

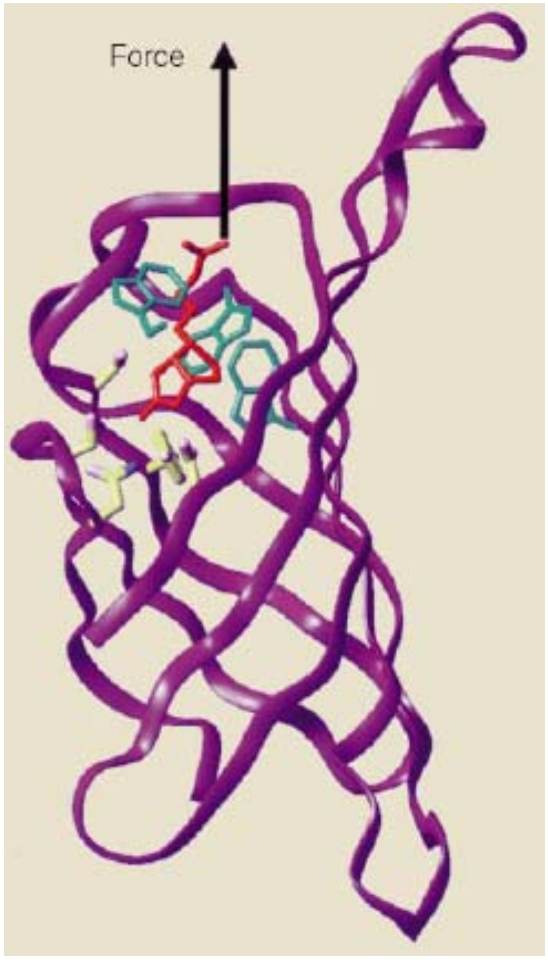

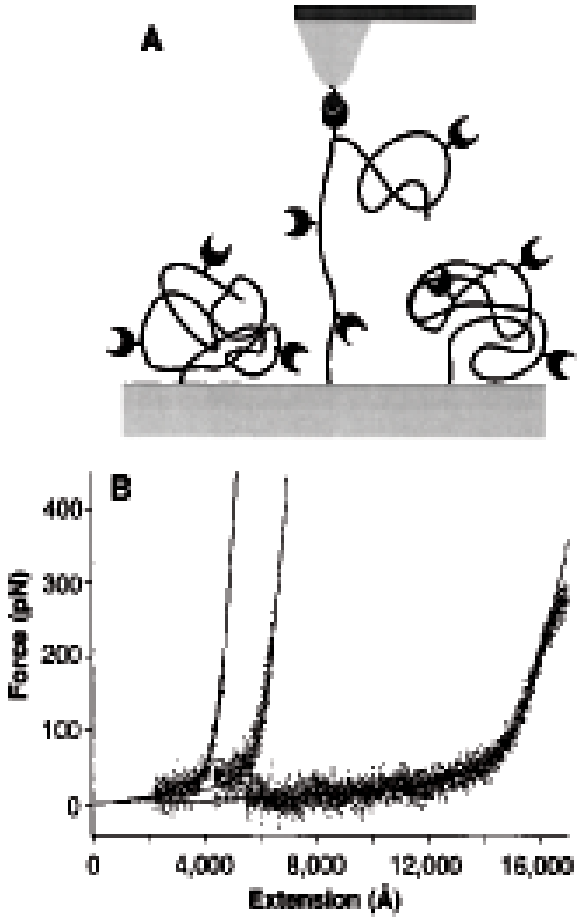

Gaub，Science paper

DNA Structural Transitions

AFM Force Spectroscopy in TRIS Buffer

Duplex poly(dA-dT)

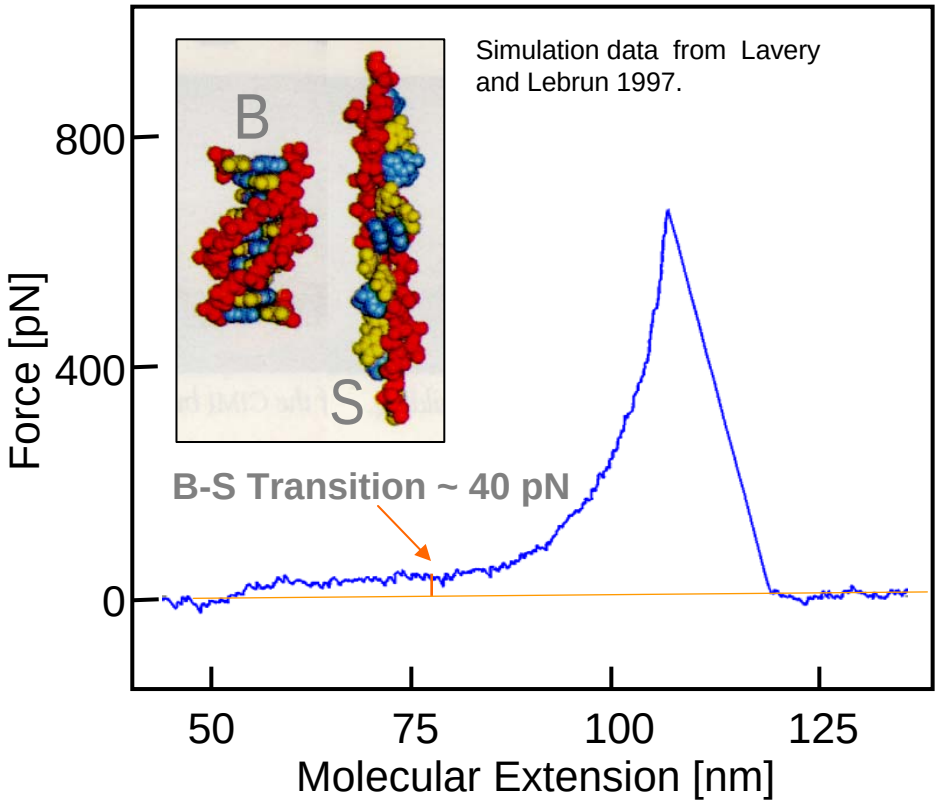

Duplex poly(dG-dC)

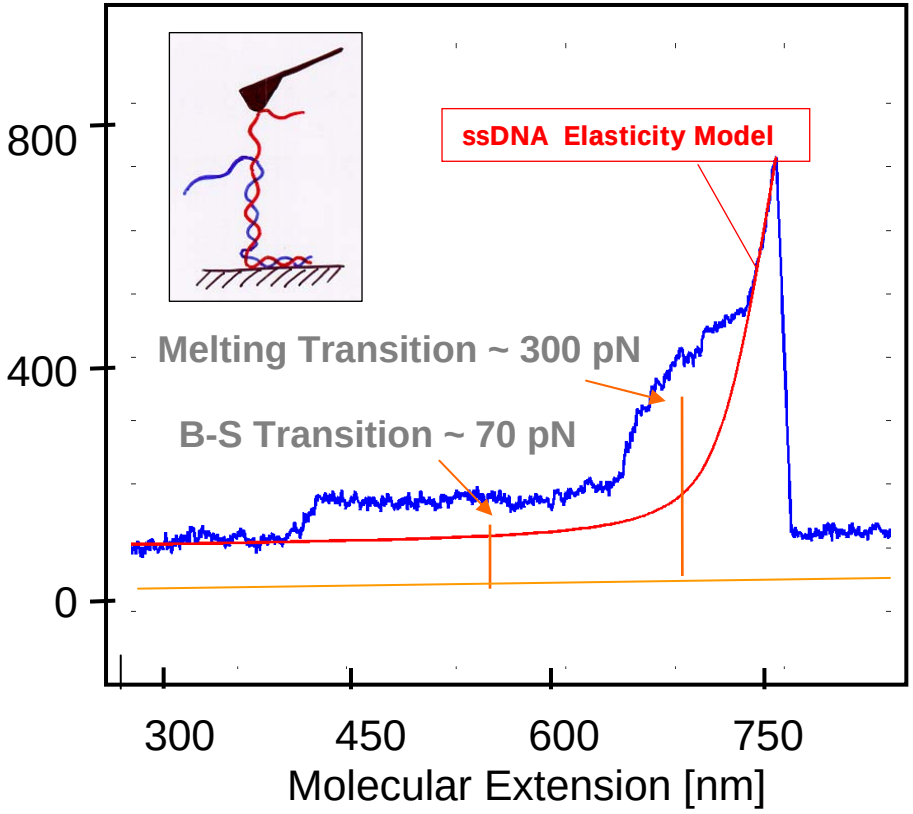

F(z) as a function of pulling speed

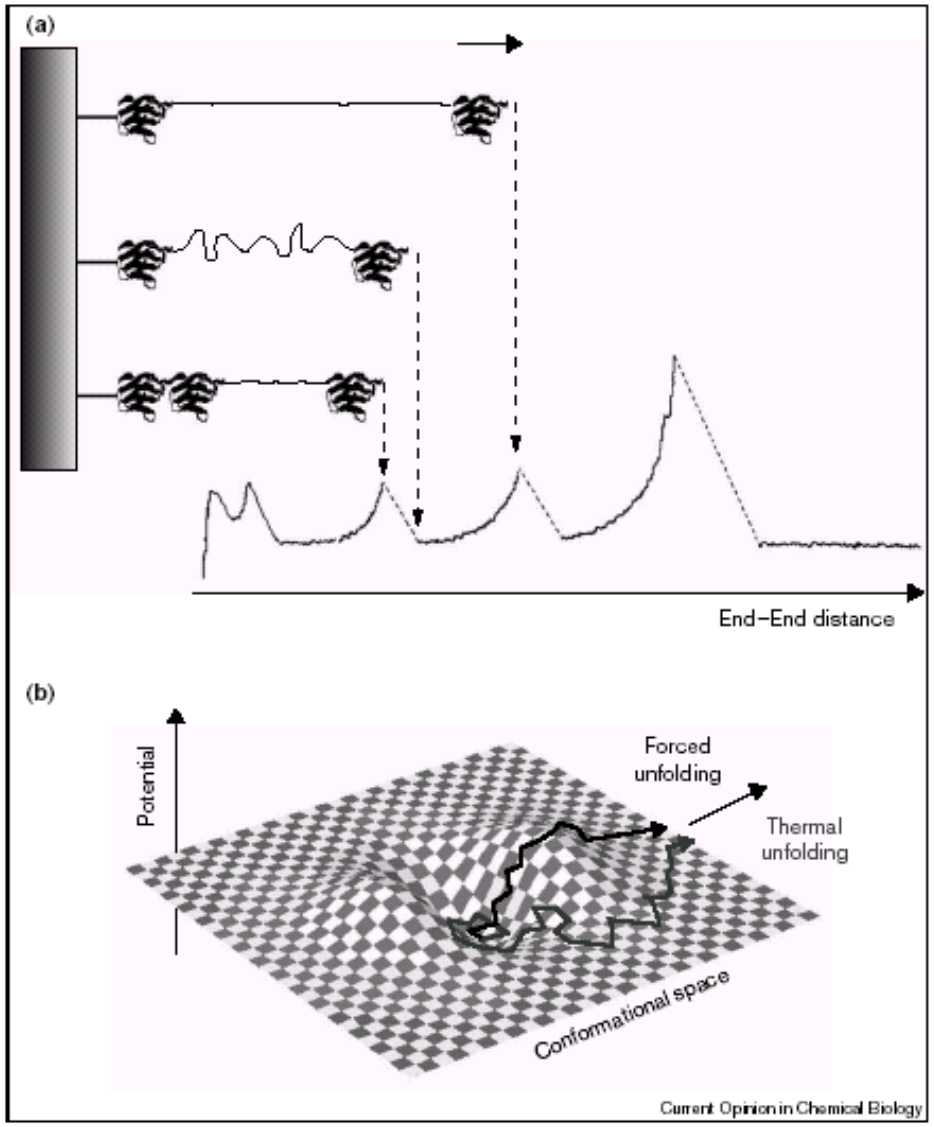

Allows the determination of energy barriers and thus is a direct measure of the energy landscape in conformational space.

Clausen-Schaumann et al., Current Opinions in Chem. Biol. **4**, 524 (2000)

Merkel et al., Nature **397**, (1999)

Evans, Annu. Rev. Biophys. Biomol. Struct., **30**, 105 (2001)

Application of AFM--lithography

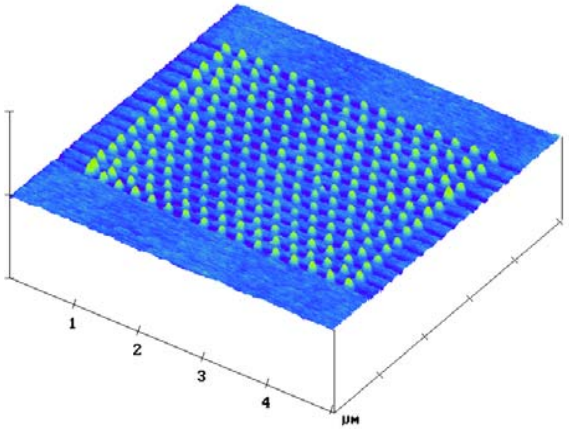

硅（111）面上的氧化硅纳米柱阵列

AFM纳米氧化刻蚀技术

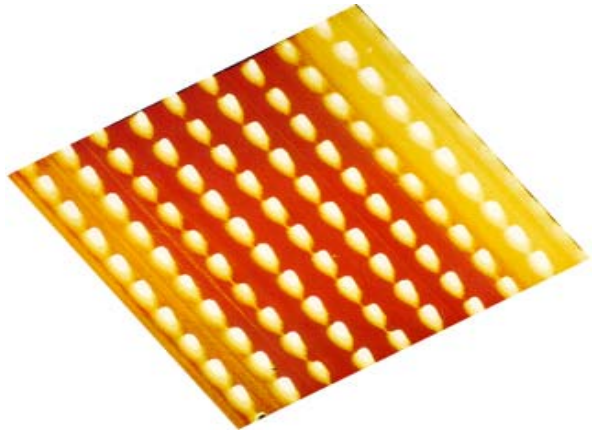

石墨上的金纳米点阵列

AFM场致蒸发技术

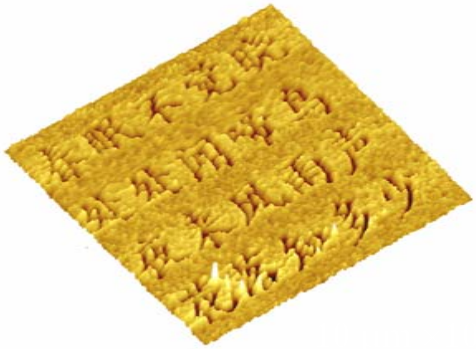

Au-Pd合金上刻写的世界上最小的唐诗

AFM机械刻蚀技术

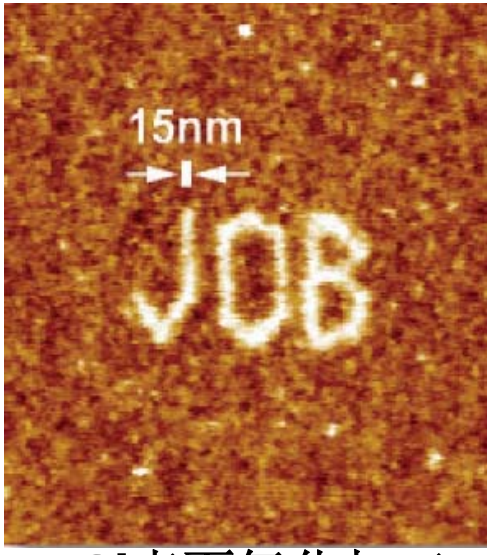

Si表面氧化加工

Application of AFM--manipulation

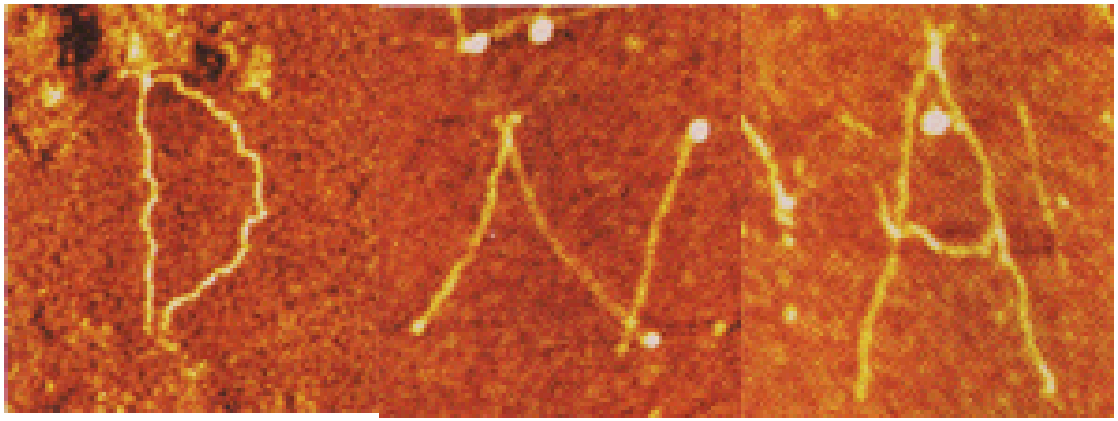

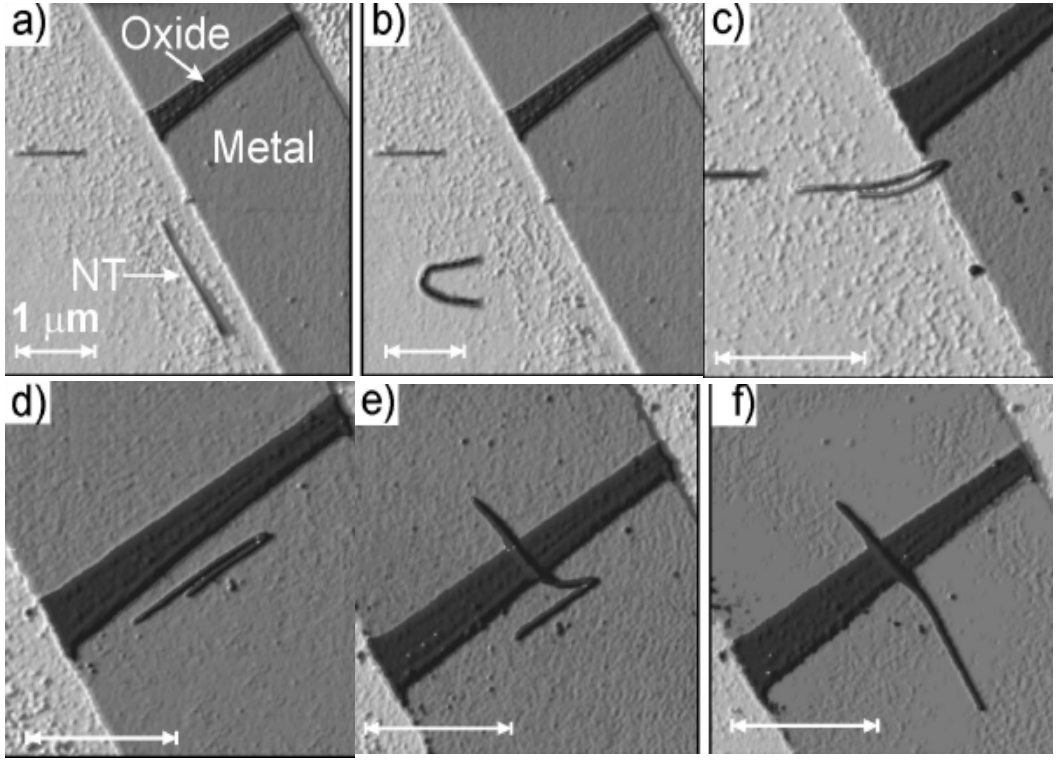

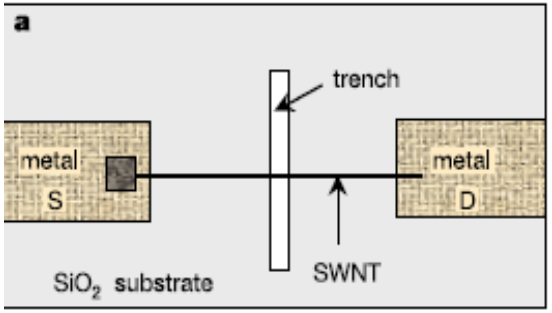

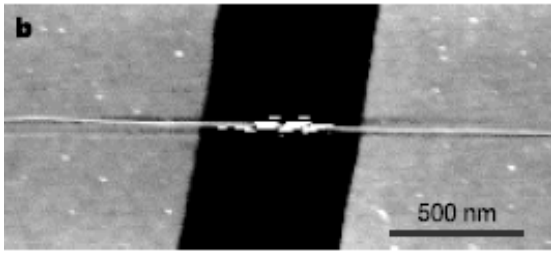

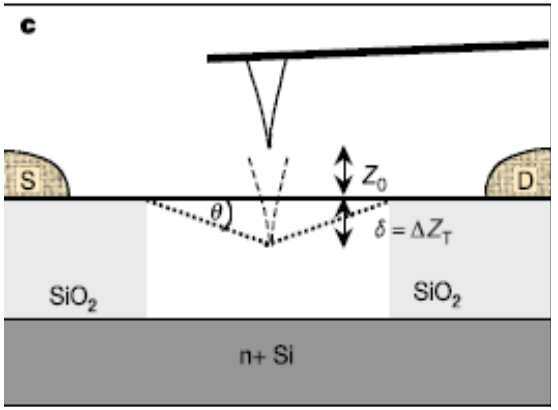

Nanoscale Three-Dimensional Patterning of Molecular Resists

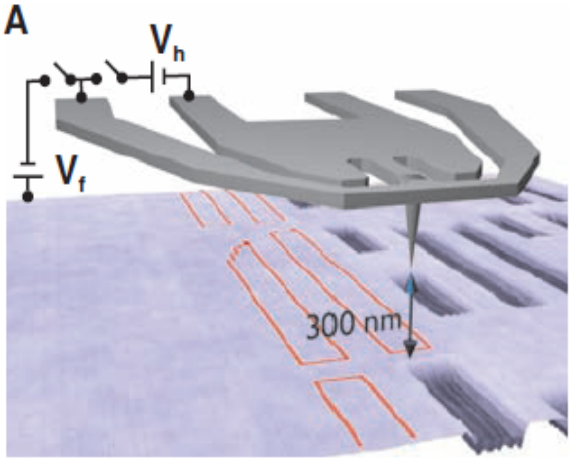

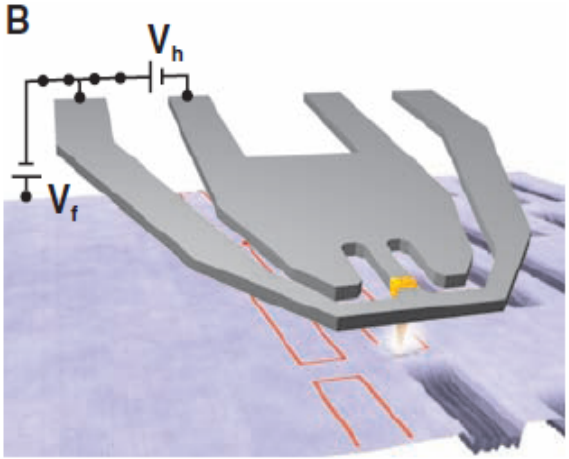

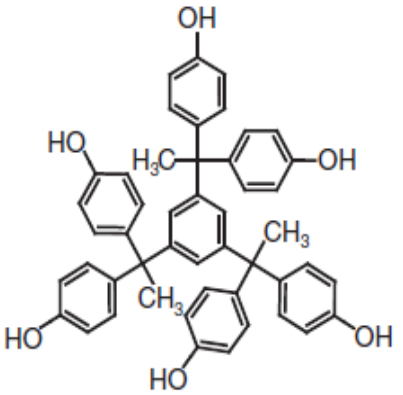

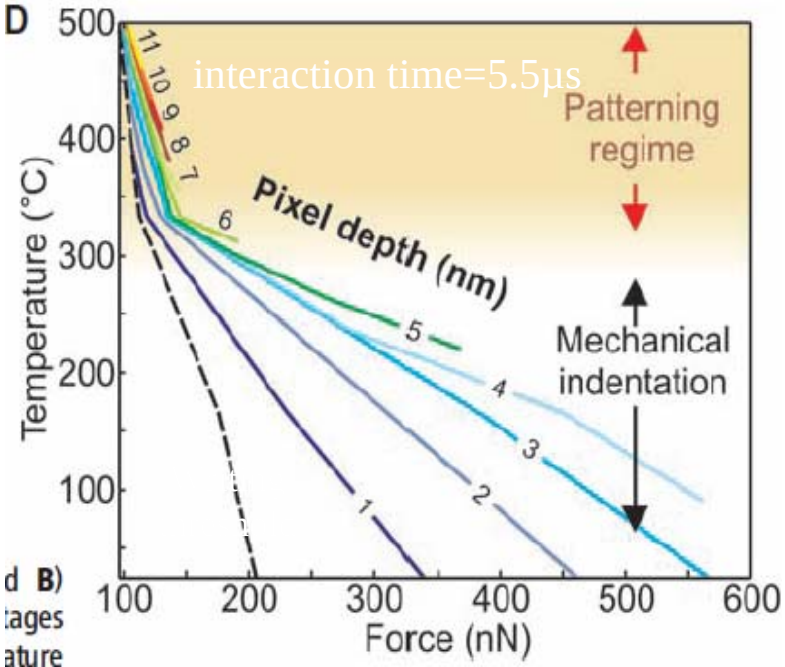

H bonds:
bound by hydrogen-bonding interactions into a glassy bulk state; provide sufficient stability for imaging and processing; sufficiently weak to be thermally activated by the hot tip.

Science 328, 732 (2010)

Nanoscale Three-Dimensional Patterning of Molecular Resists

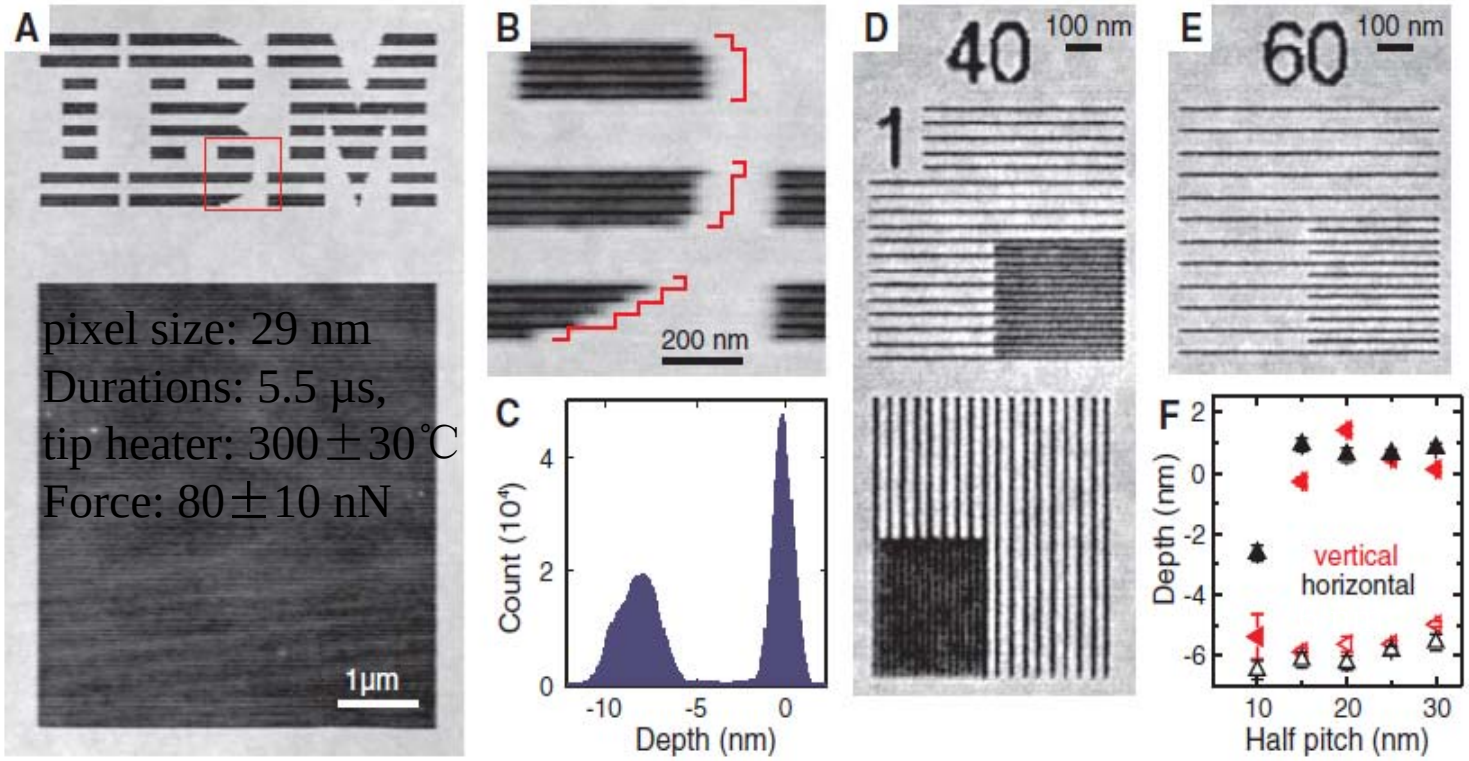

The achievable resolution increased with decreasing patterning depth.

The resolution is defined as the half pitch of fully separated dense lines,
a resolution of ~15 nm was achieved using a tip with an apex radius of ~5 nm.

Science 328, 732 (2010)

Nanoscale Three-Dimensional Patterning of Molecular Resists

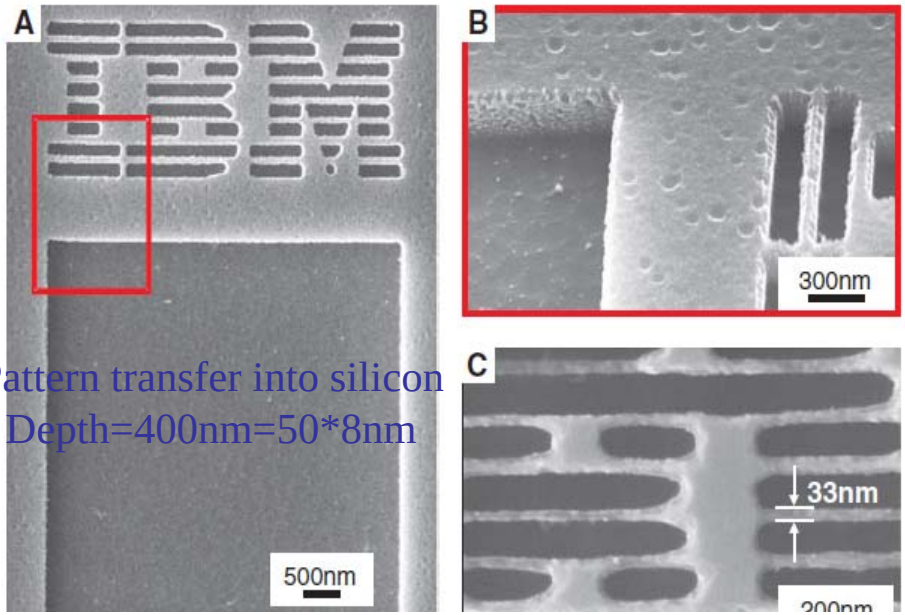

Pattern transfer into silicon
Depth=400nm=50*8nm

Science 328, 732 (2010)

Using a mixture of SF_6 and C_4F_8 as etch gas provides a height amplification of the structures into silicon by a factor of ~3

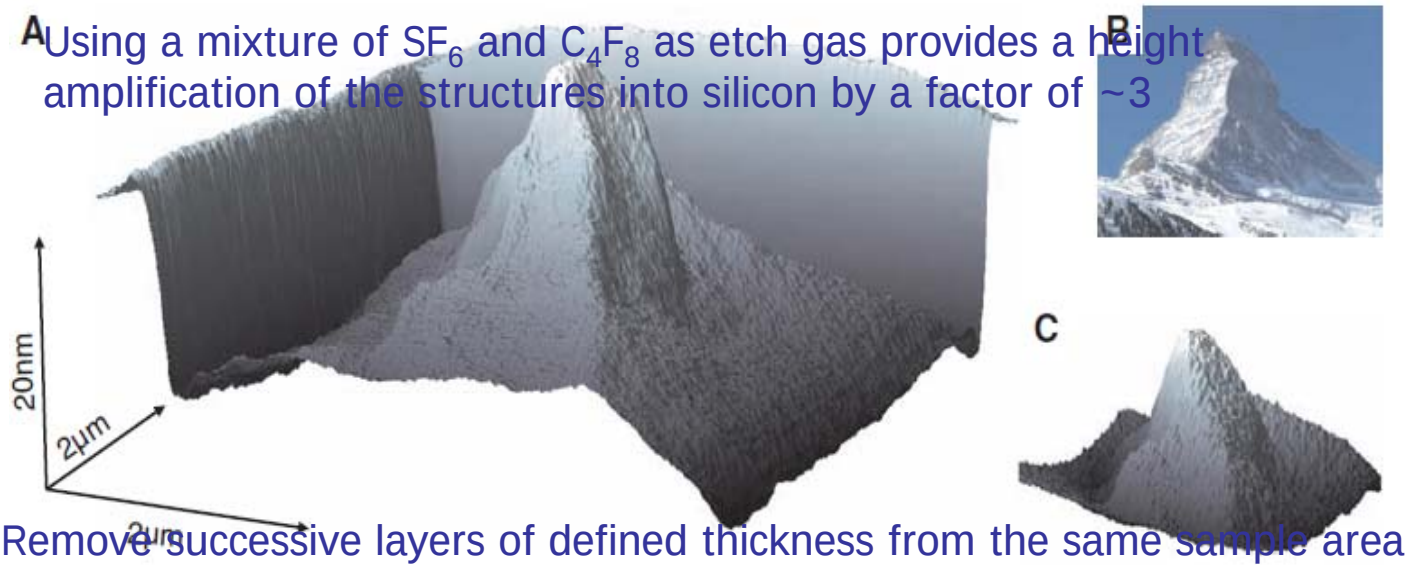

Remove successive layers of defined thickness from the same sample area

Chad A. Mirkin, Northwestern university

"Dip-pen" Nanolithography

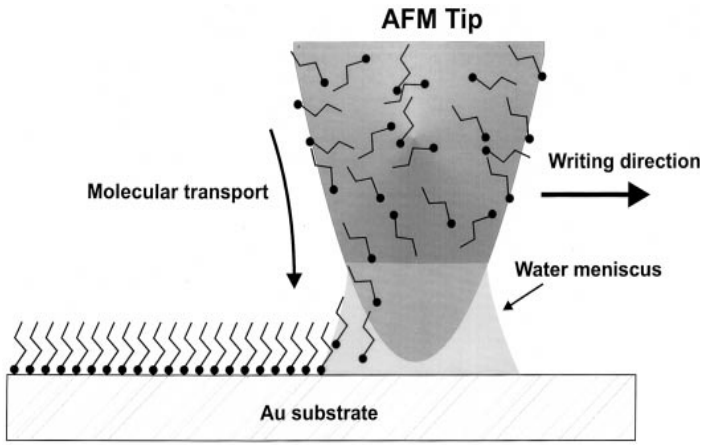

1, A silicon nitride tip was dipped into a saturated solution of ODT in acetonitrile for 1 min, coated with ODT.

2, The cantilever was blown dry.

3, Scan at the rate of 1Hz or contact with Au/mica (sp=1nN)

39%, 1Hz+4Hz

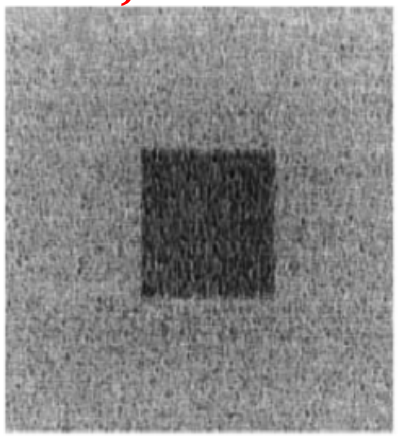

9Hz

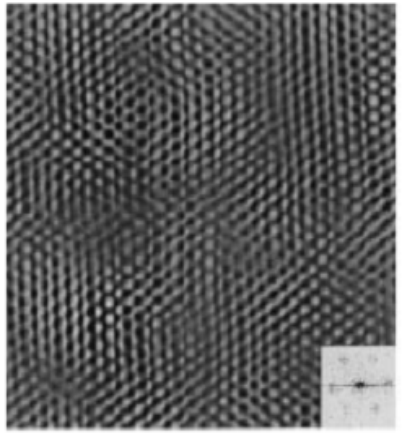

34%, 1Hz, 5min, 30nm

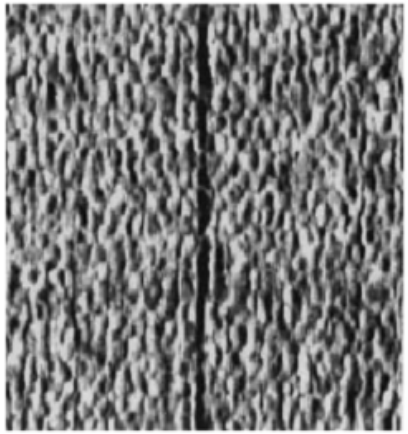

42%, 1Hz, 1.5min, 100nm

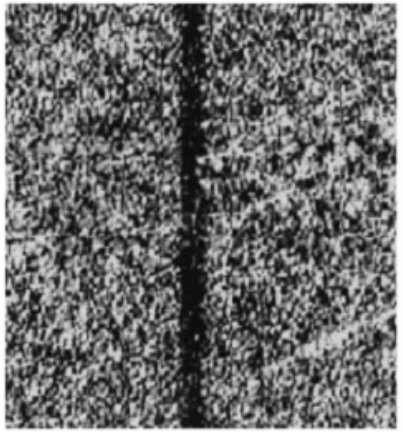

Science 283,661(1999)

lithography: parallel replication and serial writing.

Parallel replication methods :
photolithography, contact printing, and nanoimprint lithography
High throughput, but only duplicate patterns, which are predefined by serial writing approaches

Serial writing methods:
including electron-beam lithography (EBL), ion beam lithography, and many scanning probe microscopy (SPM)–based methods
create patterns with high resolution and registration but are limited in throughput

Chad A. Mirkin, Northwestern univers

Polymer Pen Lithography

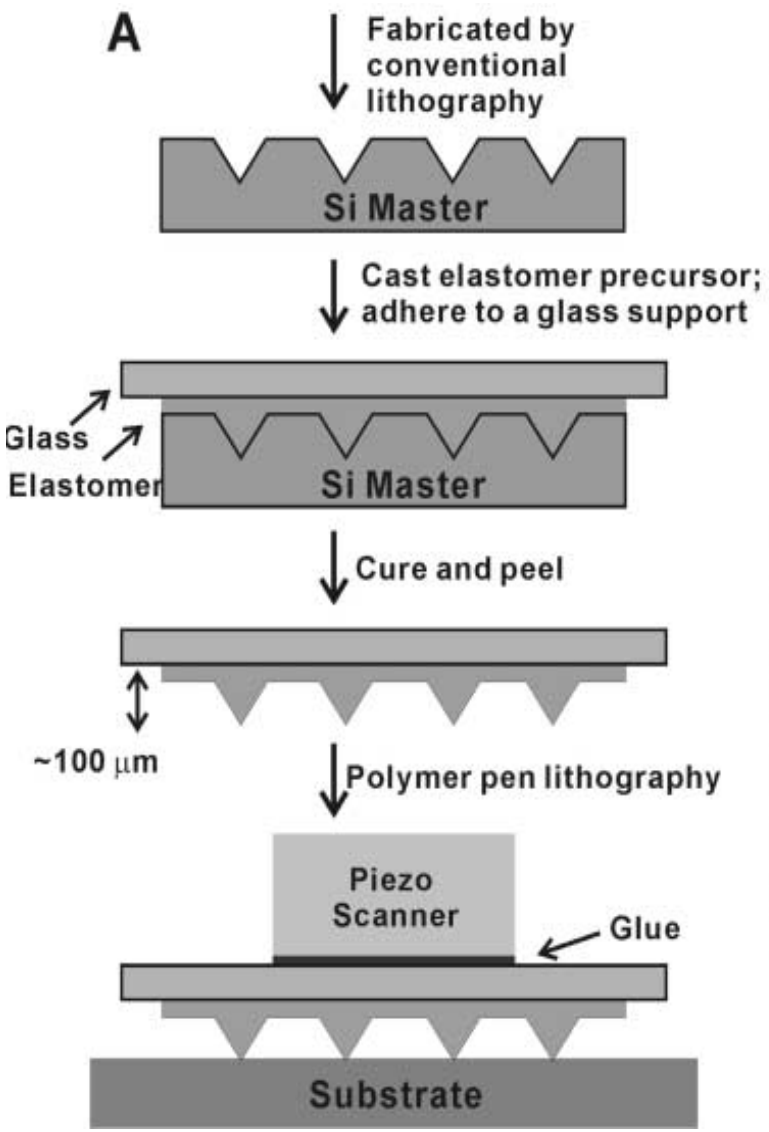

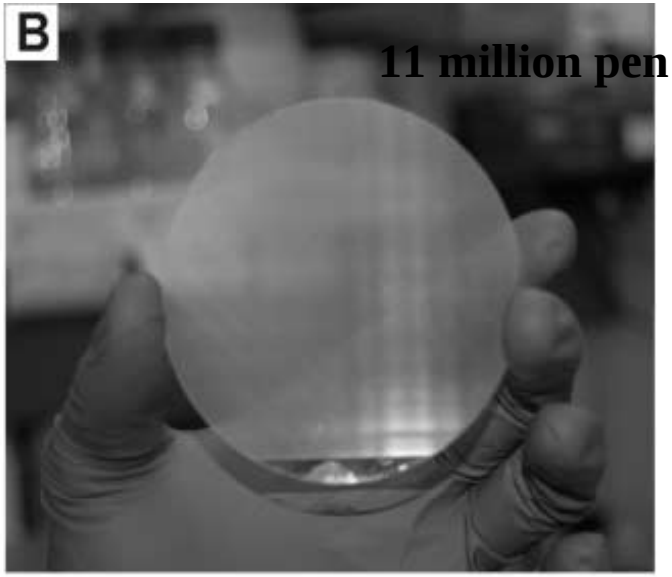

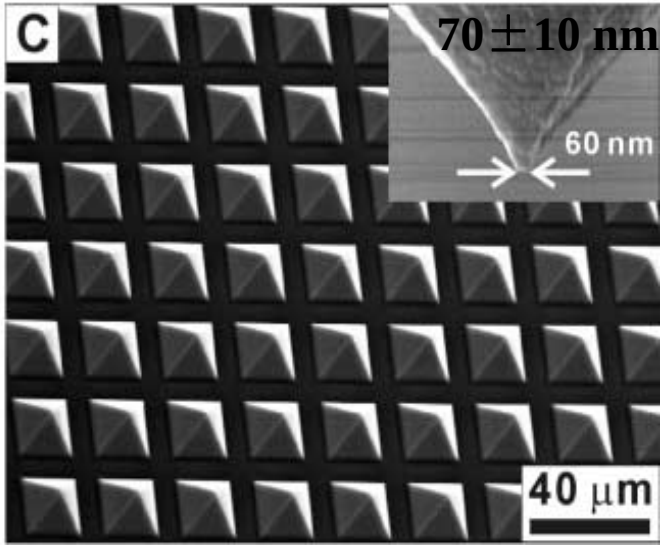

Science 321, 1658(2008)

Recipe

Ink: Immerse in a saturated solution of MHA in ethanol for 5 min followed by rinsing with ethanol,

bring in contact with the gold surface for 0.1 s to generate 1 um diameter MHA dot,

Repeat 35 times to generate a 6 by 6 array of MHA dots (< 10% deviation in diameter),

Etch the exposed gold to yield raised structures of 25 nm in height.

Polymer Pen Lithography

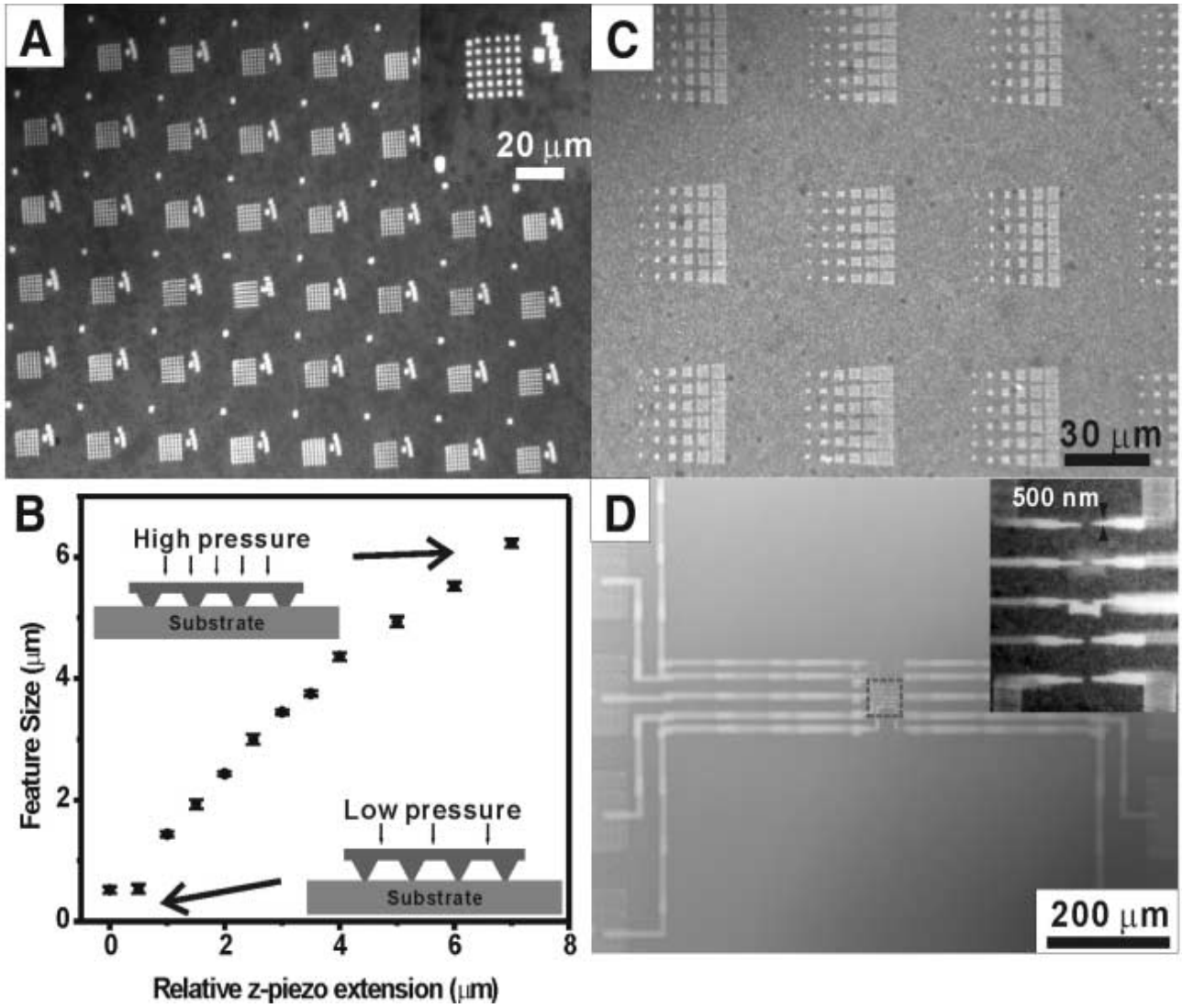

both time- and force dependent ink transport. – 纳米毛笔

Polymer Pen Lithography

15,000 replicas of the 2008 Beijing Olympic Logo

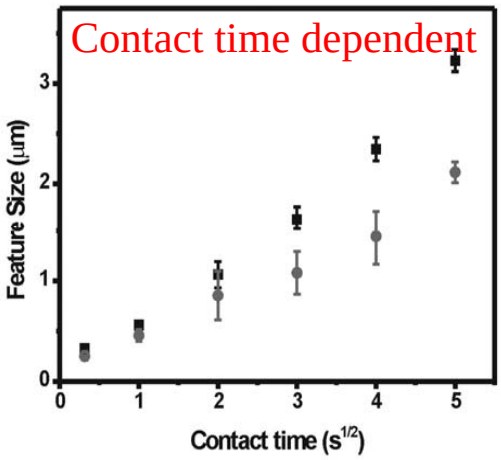

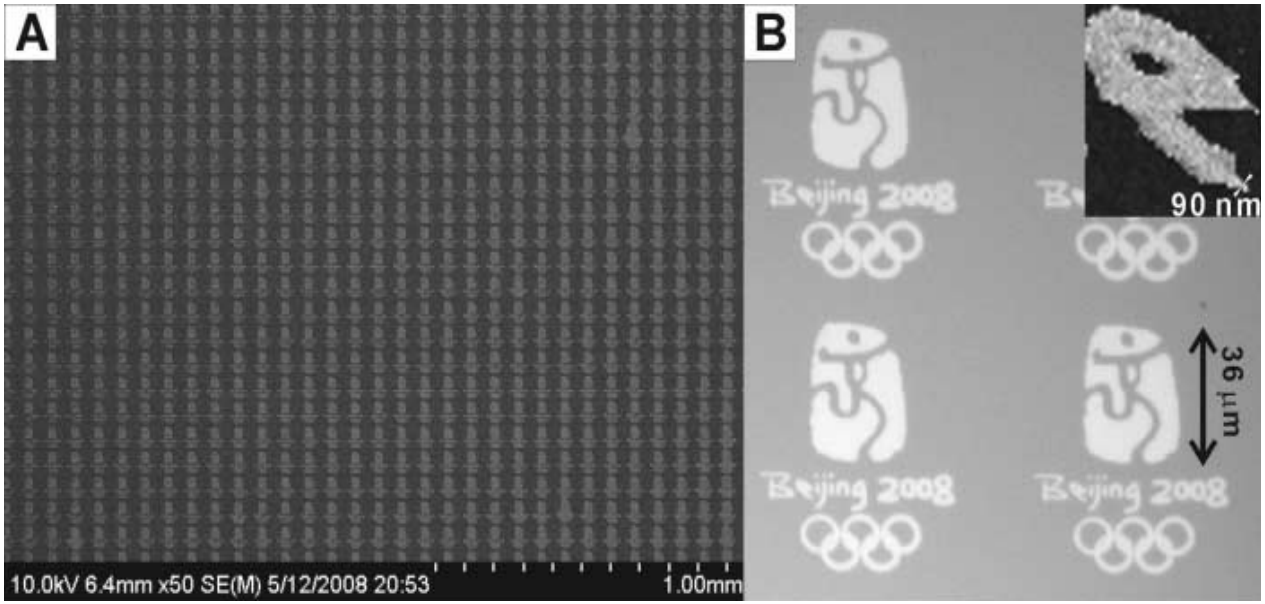

"Beijing 2008" : ~2000 90nm dots (initial contact),
the picture and Olympic rings : ~4000 600nm dots (extension =1 um).
hold the pen array at each spot for 0.05 s and travel between spots at 60 um/s.
Total time is less than 40 min.

Chad A. Mirkin, Northwestern univers

Hard tip, Soft-spring Lithograph

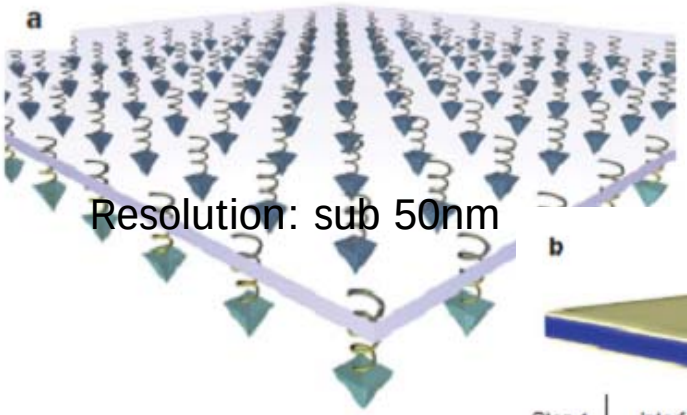

Resolution: sub 50nm

Transparent
Without laser

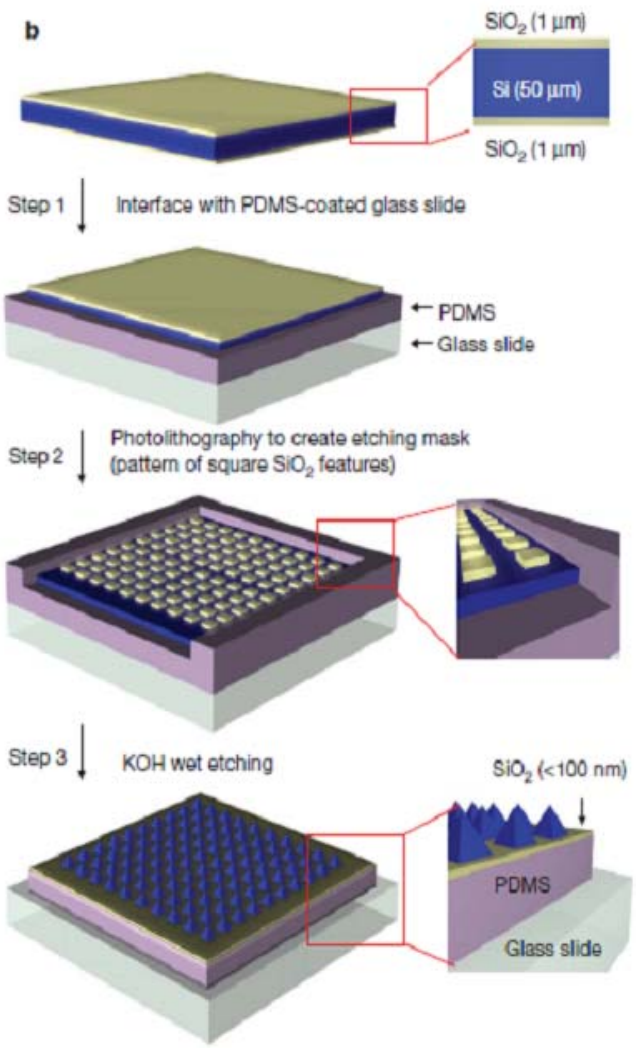

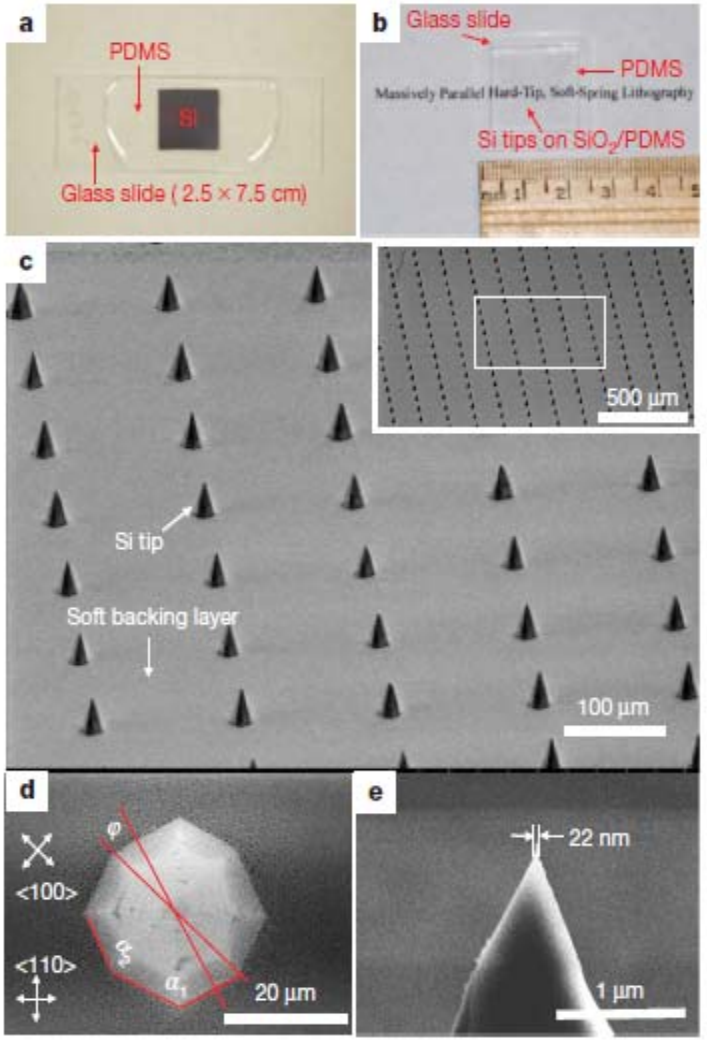

ultra-sharp Si tips on a spring-like elastomer layer that coats a glass slide
allows all of the tips to be brought into contact with a surface over large areas

Nature 469, 516 (2011

Chad A. Mirkin, Northwestern univers

Hard tip, Soft-spring Lithography

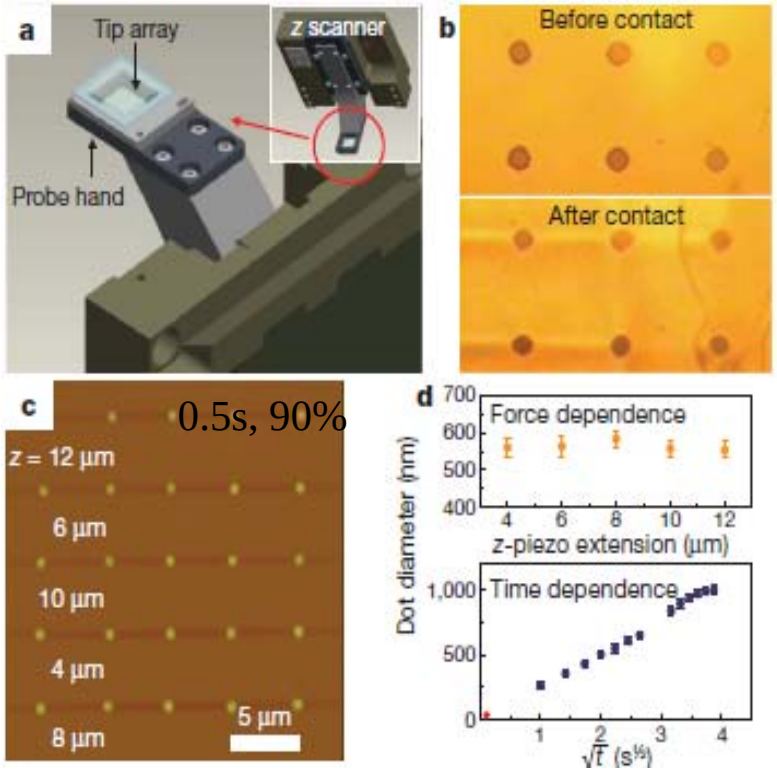

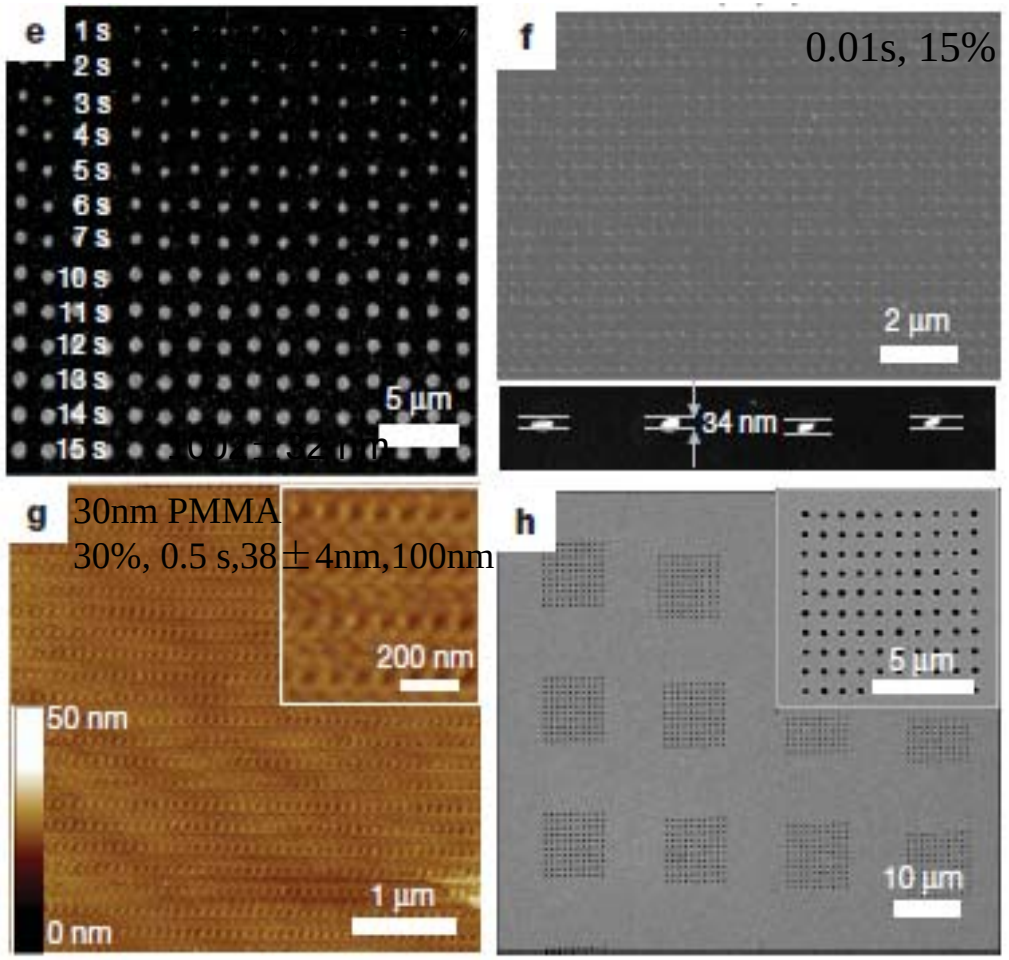

array of holes, 274±20nm

the tip arrays were coated with Au and brought into contact with MHA/Au surface

the MHA SAM was removed selectively (–5V, 5 s, 30%)

Dwell time and humidity can be used to control the feature size from several mm to less than 50nn

Hard tip, Soft-spring Lithography

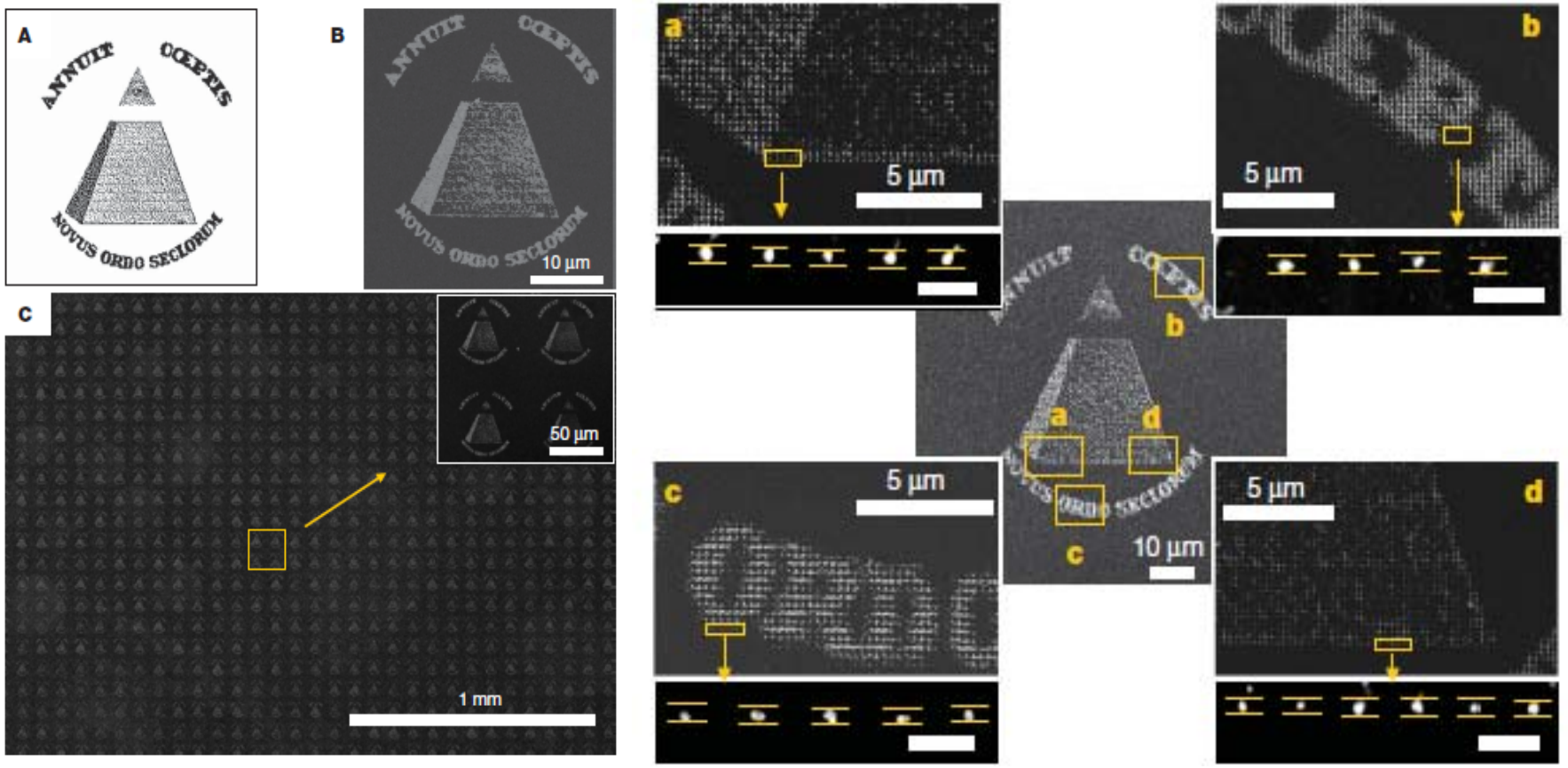

- Load the image into the AFM software, convert it into a dot-matrix representation.
- The computer generated pattern is composed of 6982 dots .
- Ink the 4750 HSL tip array (1cm×1 cm) with MHA
- Generate the etched Au dots (0.01 s, 40%).
- Obtain an accurate miniaturized duplication (30×33 μm, pitch 150nm).
  (55×60 μm, 0.01 s, 30%, 270nm)

Atomic resolution with nc- AFM

AFM's path to atomic resolution

Si(111)-(7×7)

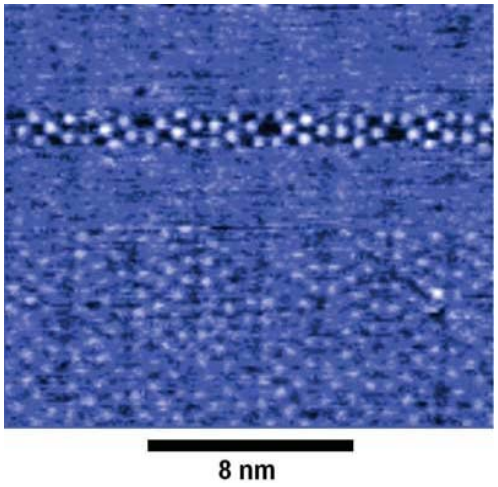

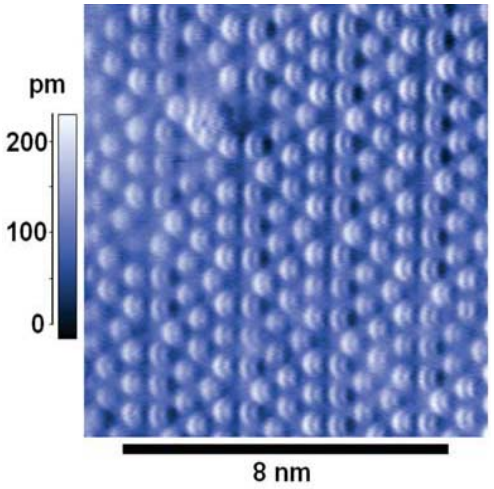

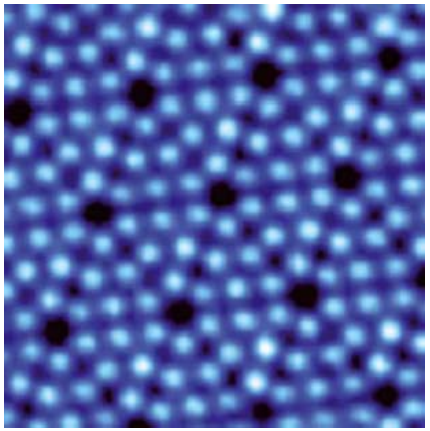

Science 267, 68(1995)

k=17 N/m
A = 34 nm
f_0 = 114 kHz
Δ f = -70 Hz
Q = 28000

Science 289, 422(2000)

k=1800 N/m
A = 0.8 nm
f_0 = 16.86 kHz
Δ f = -160 Hz
Q = 4000.

nc-AFM image of Si7x7 at low temperature
T = 2.4 K;
A = 69 pm;
Q = 80000;
Δ f = -1.3 Hz
Courtesy of Toshu An, group of Prof. Hasegawa, The University of Tokyo

AFM's path to atomic resolution

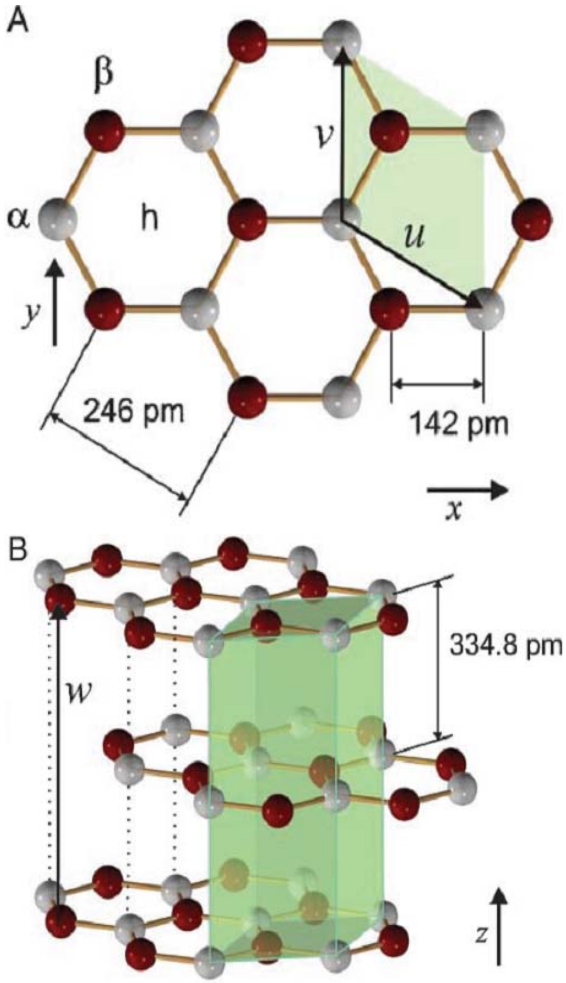

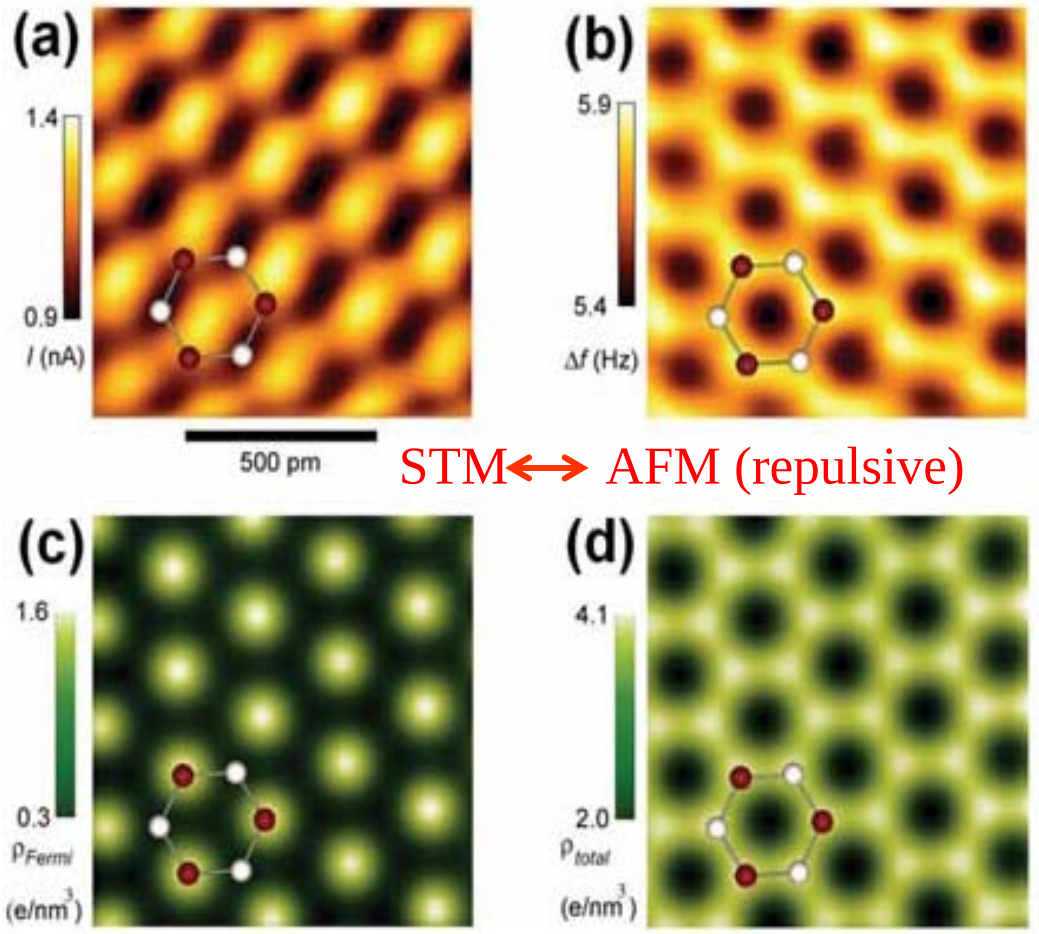

W tip; k = 1800 N/m; A = 0.3 nm; f_0 = 18076.5 Hz; Q = 20000

PNAS 100(22), 12539(2003)

AFM's path to atomic resolution

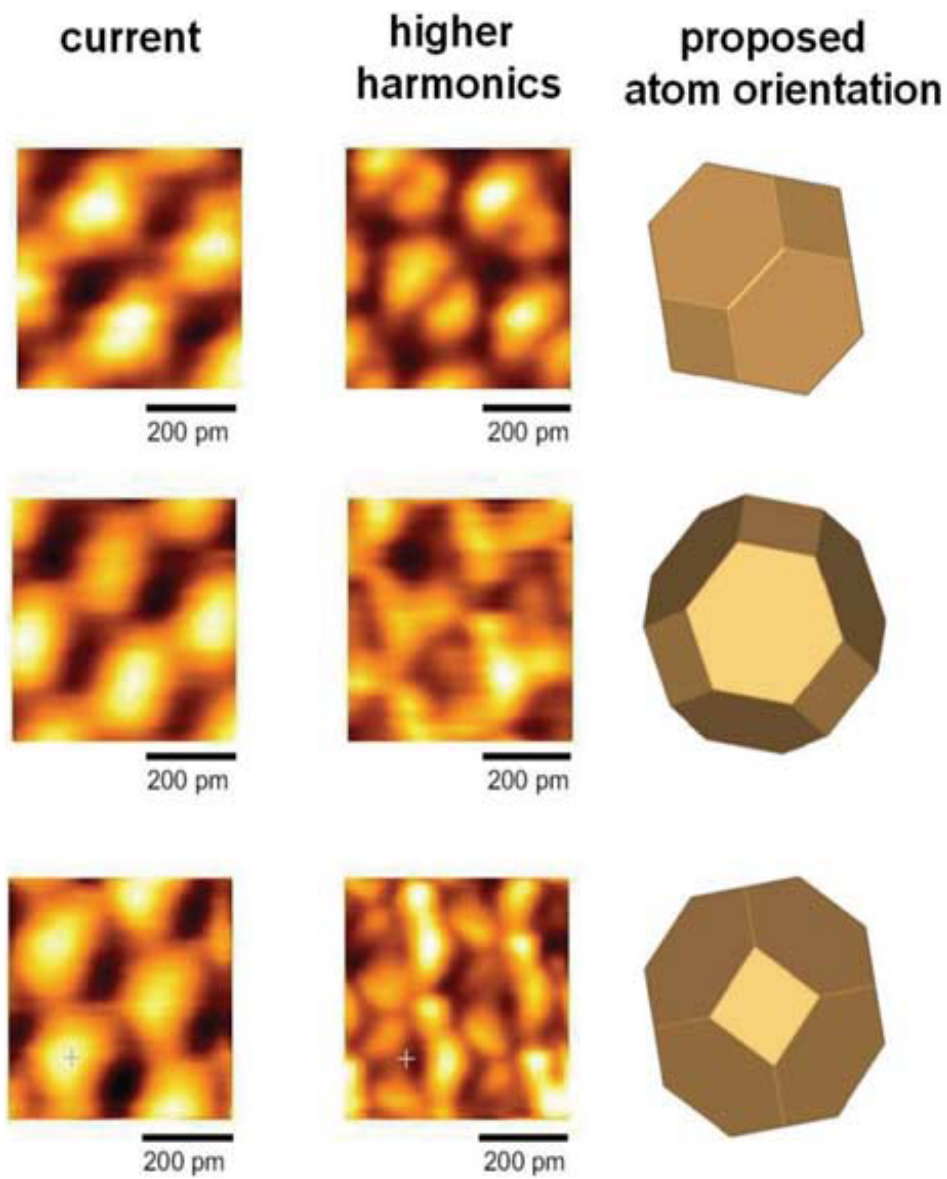

two-fold symmetry
[110] orientation

three-fold symmetry
[111] orientation

four-fold symmetry
[001] orientation

$$\frac{d^n}{dr^n}\left(\frac{1}{r^2}\right)=\frac{1}{r^{2+n}}$$

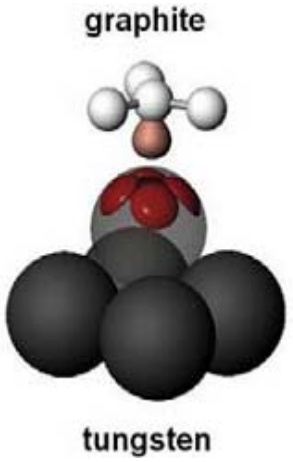

k = 1800 N/m
A = 0.3 nm
f_0 = 18076.5 Hz
Q = 20000
T = 4.9 K

Science 305, 380(2004)

Figure 3: Pentacene imaged with STM and NC-AFM.

From

Recent advances in submolecular resolution with scanning probe microscopy

Leo Gross

Nature Chemistry **3**, 273–278 (2011) | doi:10.1038/nchem.1008

Published online 24 March 2011 | Corrected online **08 April 2011**

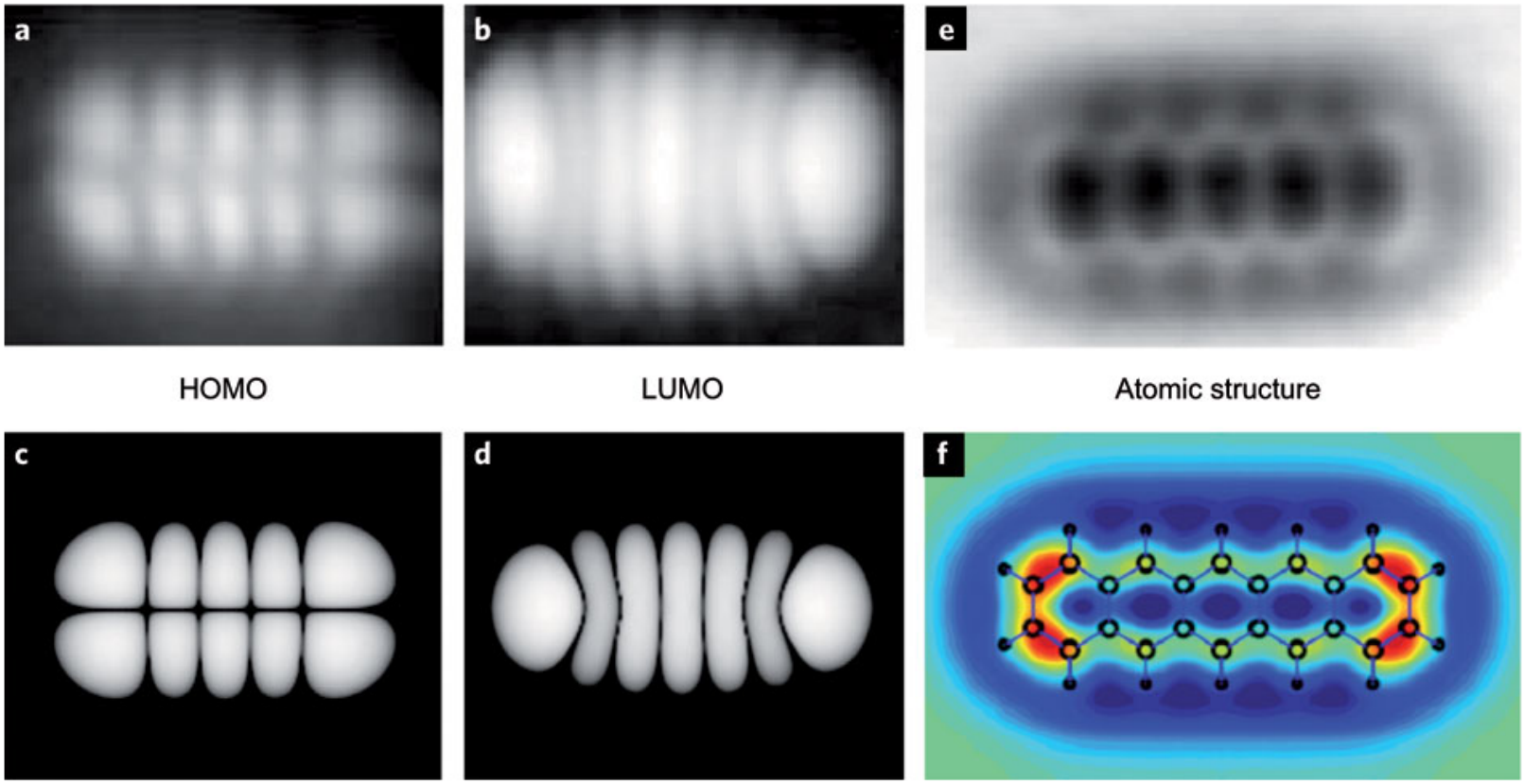

a,b, Molecular orbital images of pentacene on two monolayer NaCl on Cu(111) obtained by STM using a pentacene-terminated tip. Image size 2.5 nm × 2.0 nm; constant current. The HOMO (**a**) was imaged by setting the sample voltage to the first resonance at negative bias at V = −2.5 V, thus tunnelling out of the molecular orbital. The LUMO (**b**) is imaged by electrons tunnelling from the tip into the orbital at positive bias *V* = +1.7 V. c,d, Contours of constant orbital probability distribution of the HOMO (**c**) and LUMO (**d**) of the free pentacene molecule obtained by DFT. **e**, NC-AFM image of pentacene on two monolayer NaCl on Cu(111) obtained using a CO-functionalized tip. Image size 2.2 nm × 1.4 nm; oscillation amplitude *A* = 0.07 nm. **f**, Computed frequency shift for an intermolecular distance *d* = 0.475 nm between CO and pentacene. Reprinted with permission from: **a–d**, ref. 9, © 2005 APS; **e**, ref. 1, © 2009 AAAS; f, ref. 34, © 2010 IOP.

The chemical structure of a molecule resolved by AFM

Cu(111)

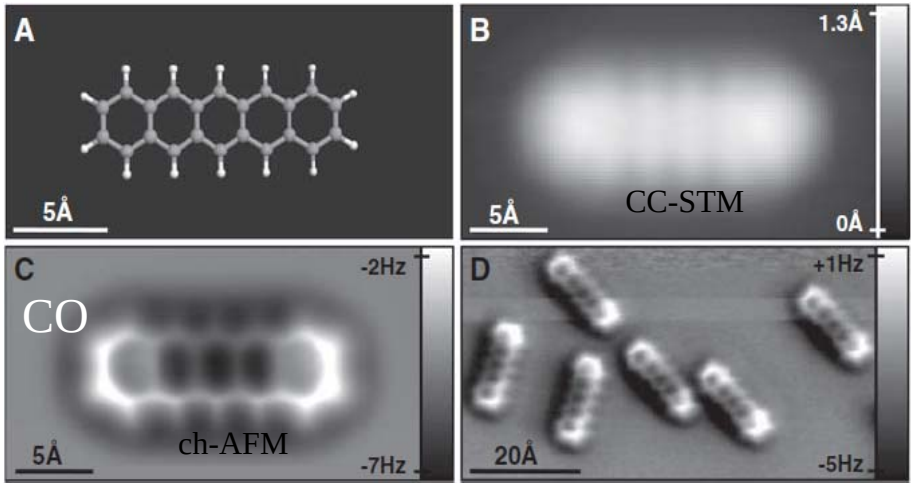

CO-terminated tip

NaCl(2ML)/Cu(111)

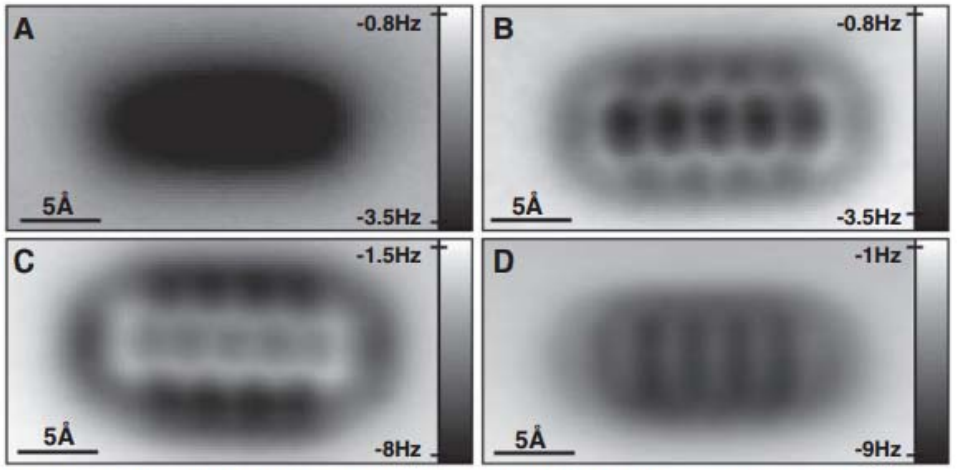

Fig. 2. Constant-height AFM images of pentacene on NaCl(2ML)/Cu(111) using different tip modifications (*16*). (**A**) Ag tip, $z = -0.7$ Å, $A = 0.6$ Å; (**B**) CO tip, $z = +1.3$ Å, $A = 0.7$ Å; (**C**) Cl tip, $z = -1.0$ Å, $A = 0.7$ Å; and (**D**) pentacene tip, $z = +0.6$ Å, $A = 0.5$ Å. The z values are given with respect to a STM set point of $I = 2$ pA, $V =$ 200 mV above the NaCl(2 ML)/Cu(111) substrate.

Noted: Constant height image !

$\Delta f(x, y)$:

local maxima, above the edges of the hexagons, near the carbon atom

local minima, above the centers of the carbon rings (hollow sites)

Each molecule is surrounded by a dark halo.

Science 325, 1110 (2009)

Gerhaed Meyer, IBM research-Zuric

Δ f(x,y,z) and F(x,y,z)

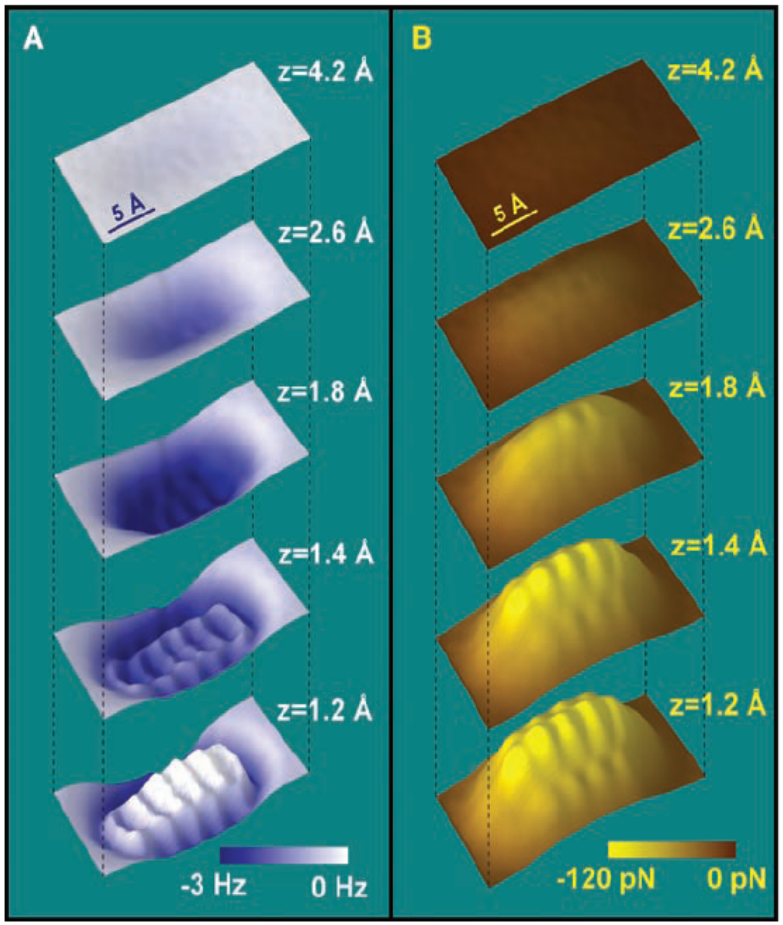

Long range force

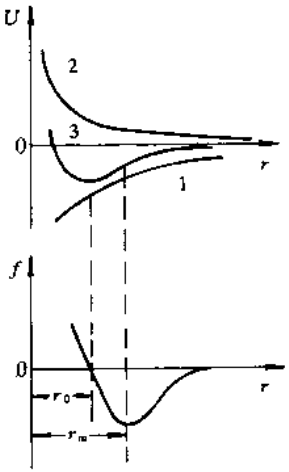

图 8-5　原子间的相互作用

Maximum attractive force

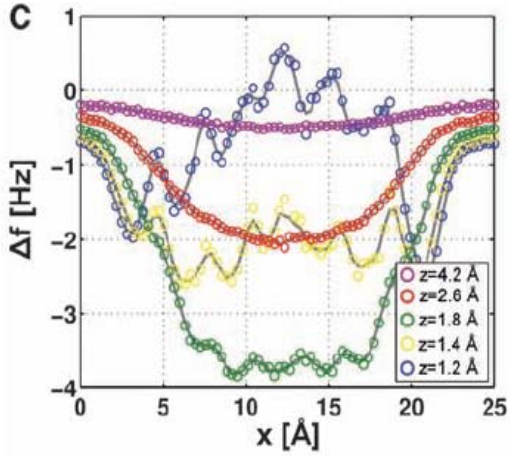

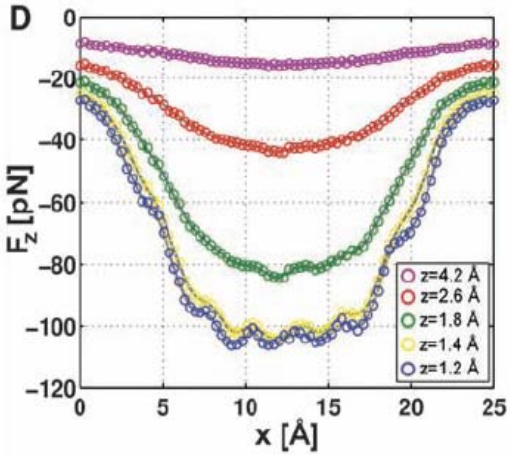

Science 325, 1110 (2009)

DFT results

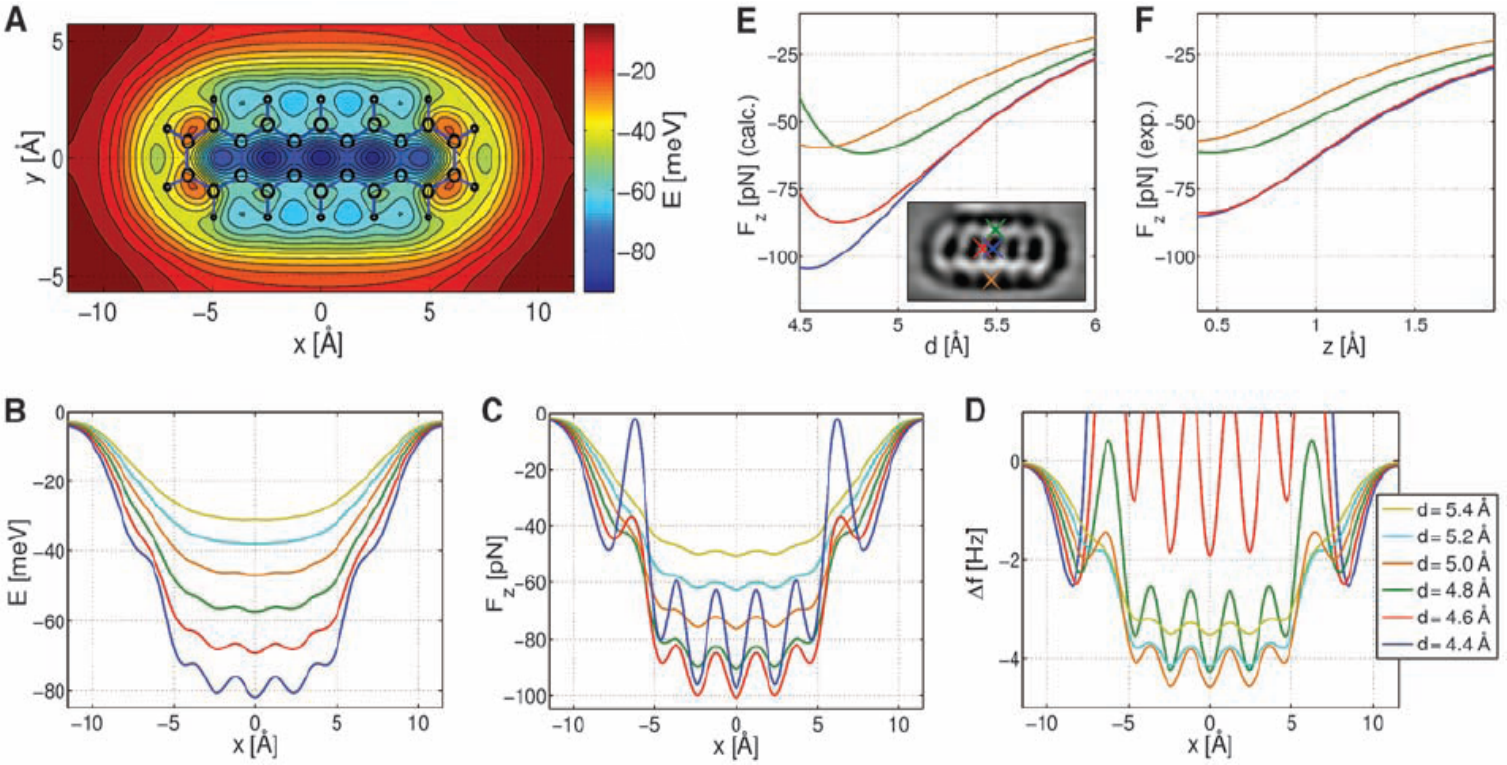

• measured the force acting on a purely metallic tip

• picked up a CO molecule and measured the force again under otherwise identical conditions.

The metallic part of the tip contributed about 30% to the attractive forces and gave no corrugation on the atomic scale

➢ Atomic resolution can only be achieved by entering the regime of repulsive forces.

➢ The vdW and electrostatic forces only contribute a diffuse attractive background with no atomic scale contrast.

➢ Modifying the tip with suitable atomic or molecular terminations is required to allow the AFM to be operated in this regime while maintaining stable imaging conditions.

Science 325, 1110 (2009)

Resolving hydrogen bond

ncAFM of 8-hydroxyquinoline (8-hq) molecule on Cu(111)

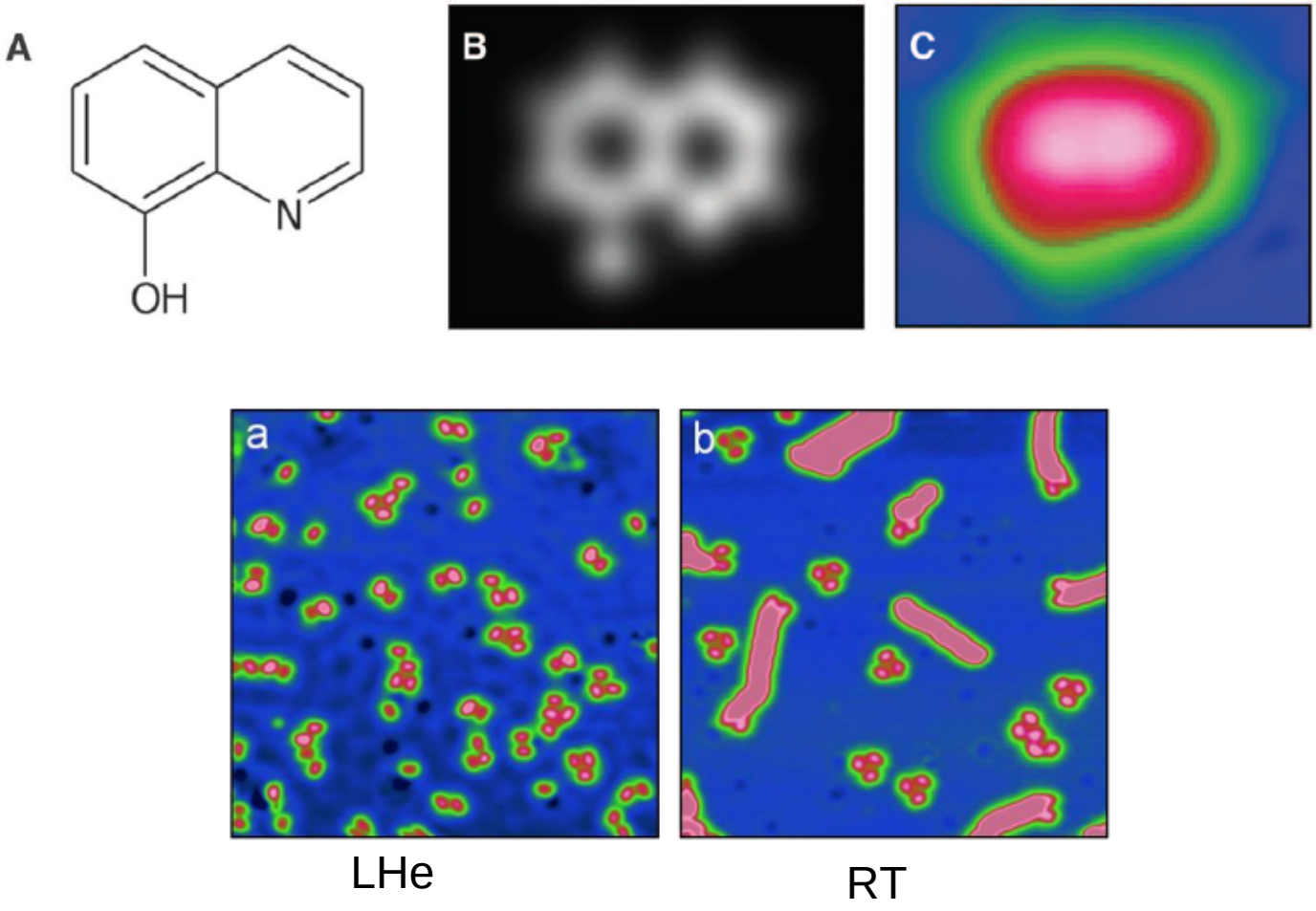

J. Zhang et al. Science 342, 611(2013)

Constant height AFM images

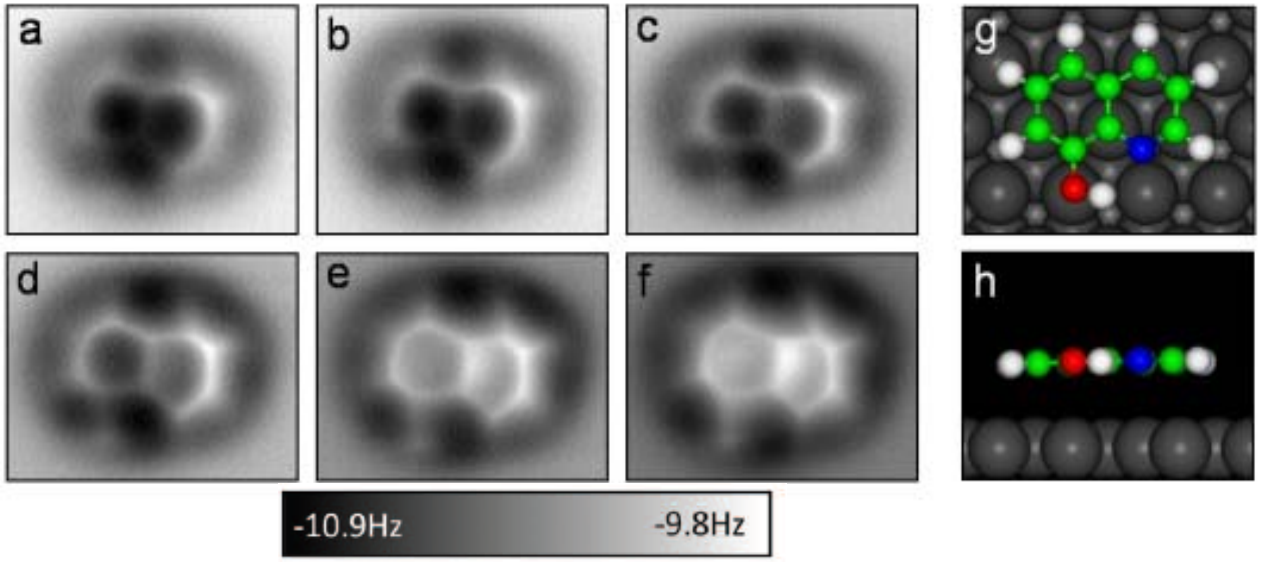

AFM sensor measured the total force of three components
(i) *long-range attractive electrostatic forces*, responsible for the overall negative Δf background
(ii) *The attractive van der Waals force*, which contributed to the dark halo surrounding the molecule without atomic corrugation
(iii) *the short range Pauli repulsion*, which contributed to the atomic contrast of molecular structure with respect to the metal substrate

J. Zhang et al. Science 342, 611(2013)

Visualizing hydrogen bonds

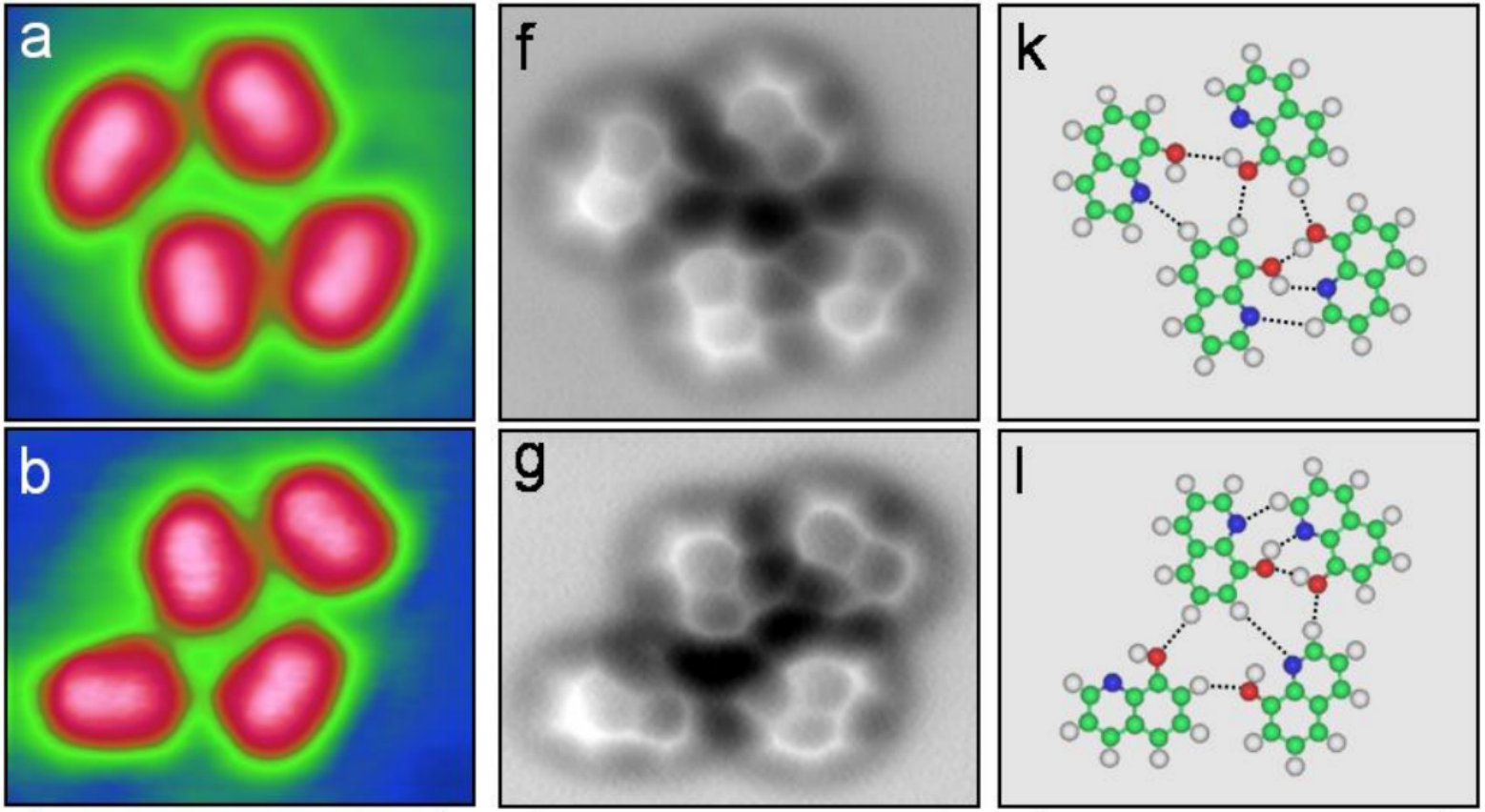

H bond has both
an electrostatic origin and a partly covalent character

Two types of hydrogen bonds

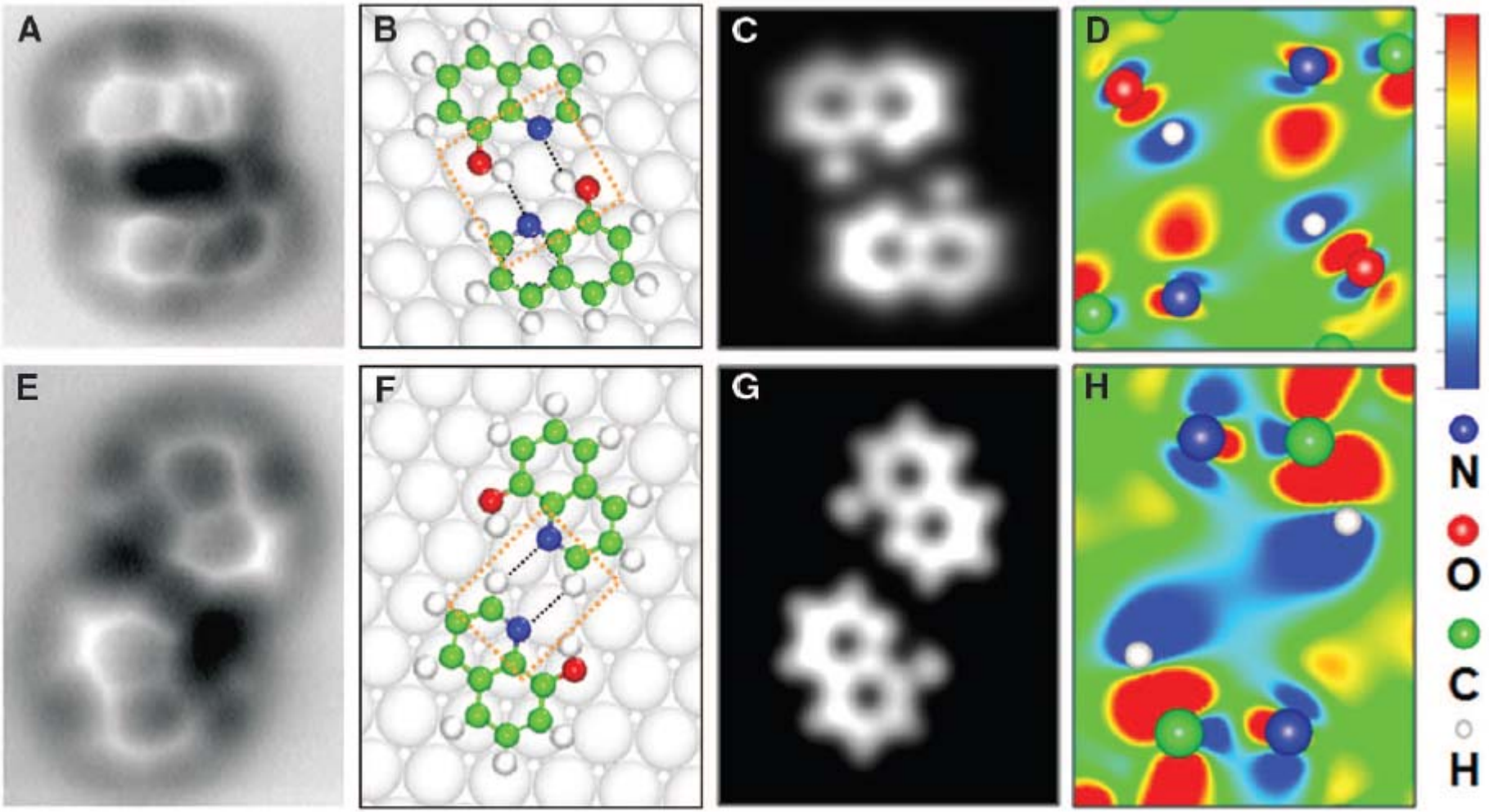

O-H···N dimer (A) – partially covalent bond character

N···H-Ph dimer (Ph, phenyl) (E)

dehydrogenated 8-hq radical

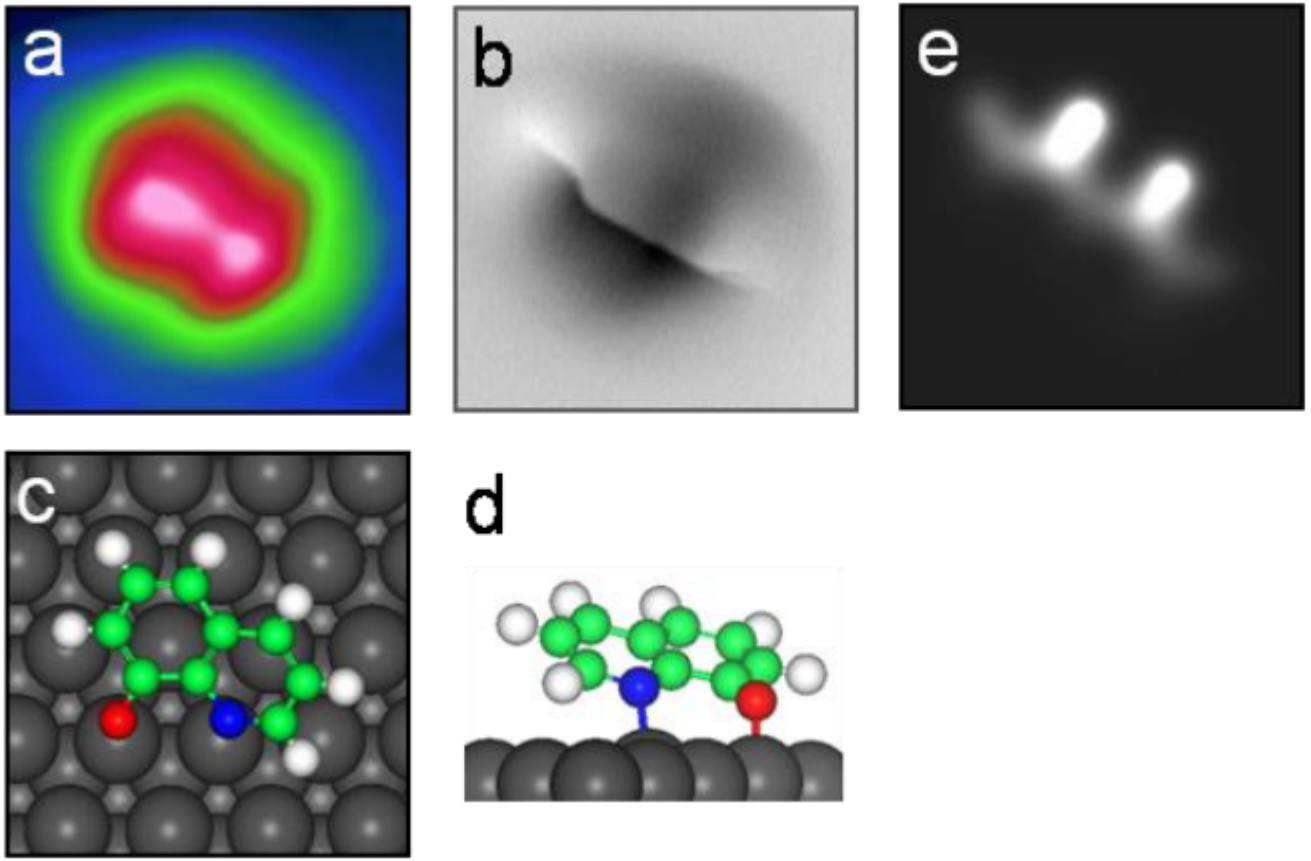

The dehydrogenation reaction takes place at room temperature due to the thermal excitations. At LHe temperature, the -OH group of 8-hq can also be dehydrogenated by a voltage pulse of ~ 3V in the vicinity of 8-hq molecule. The STM and AFM measurements on this dehydrogenated 8-hq radical indicated a molecular species with stronger tilting configuration.

Covalent bond in organometallic complex

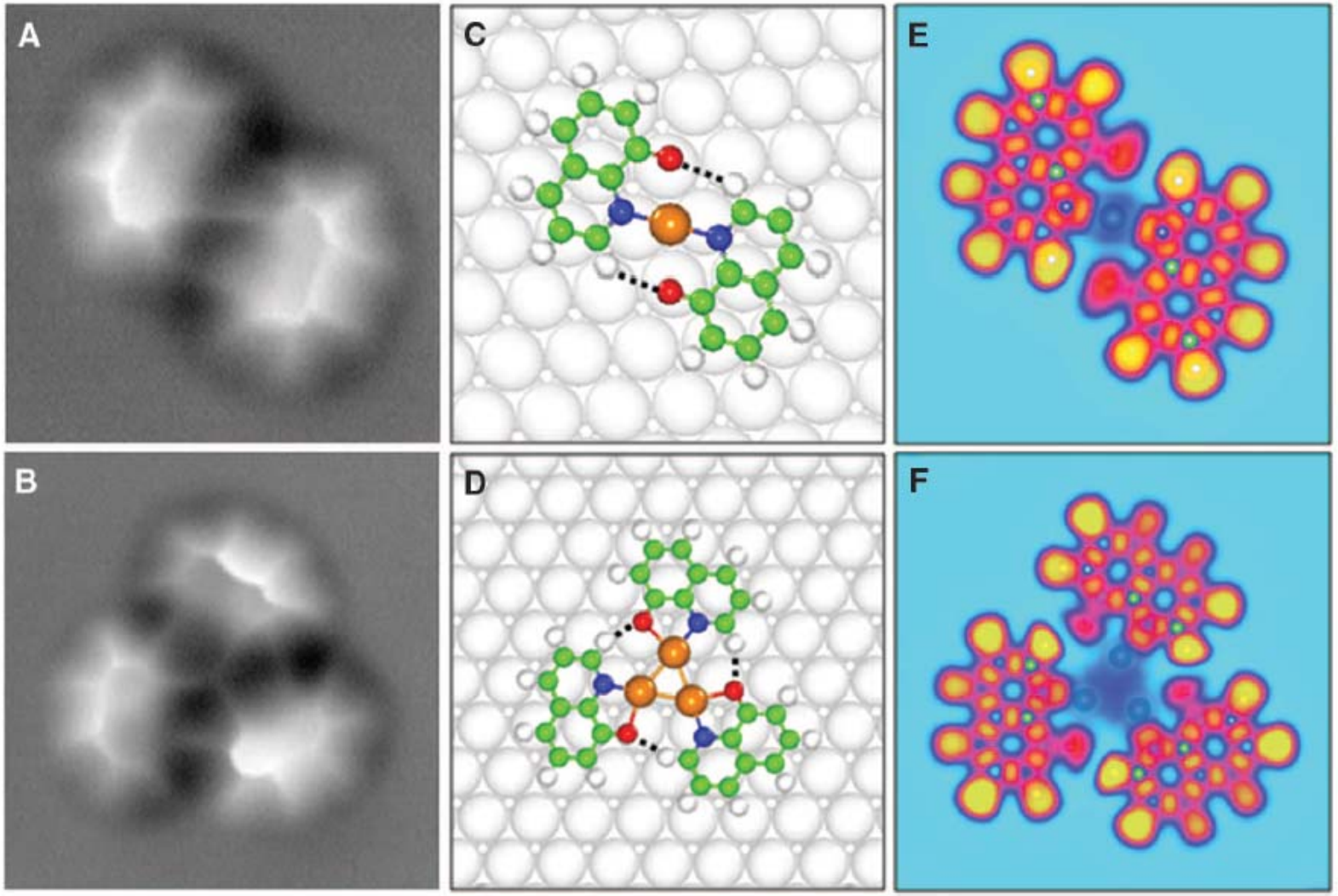

Other atomic resolved applications

Seizo Morita & Óscar custance, Osaka university, Japan

Chemical identification of individual surface atoms

Dynamic mode

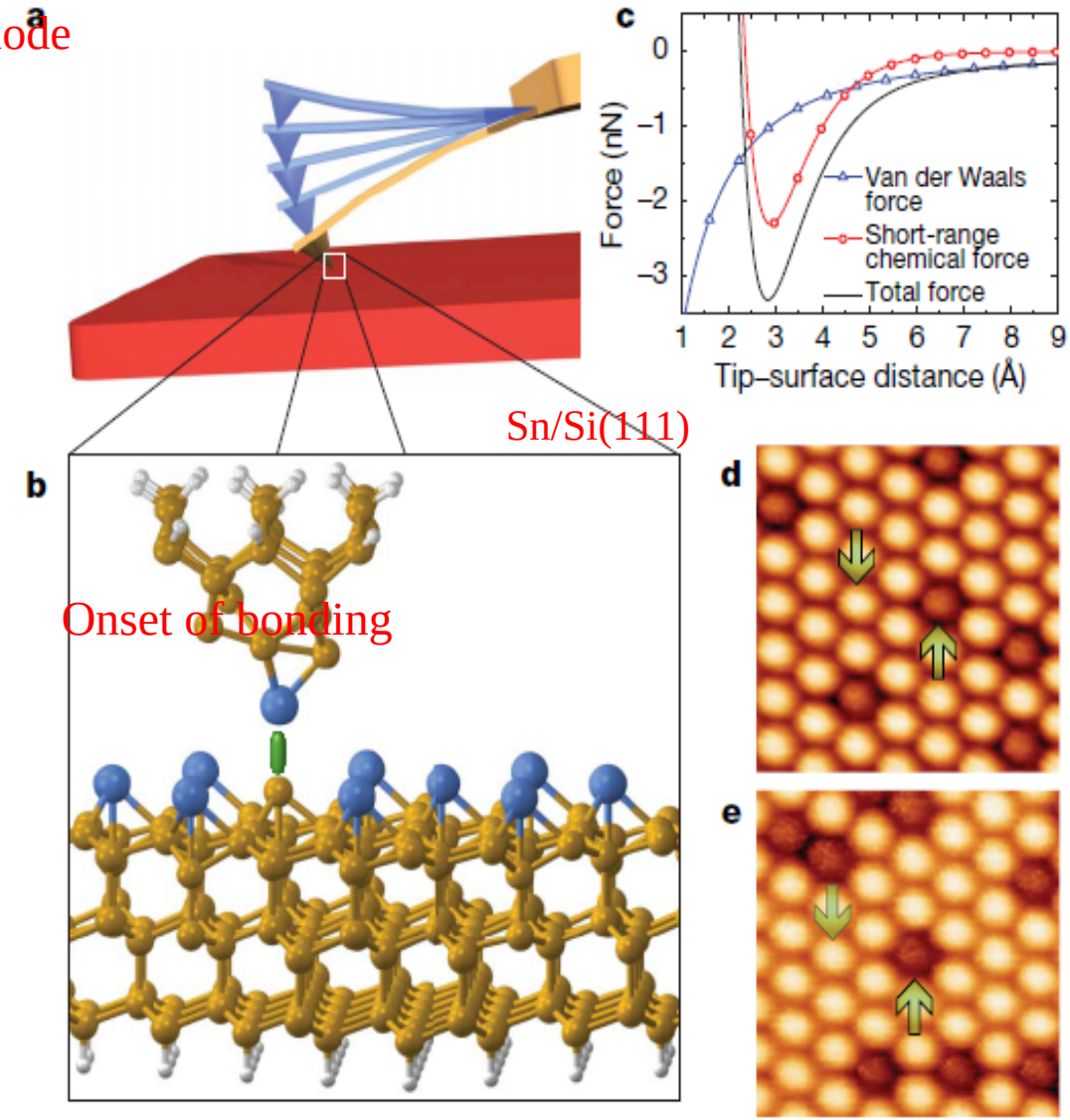

Si defects

Pb/Si(111)

Nature 446, 64 (2007)

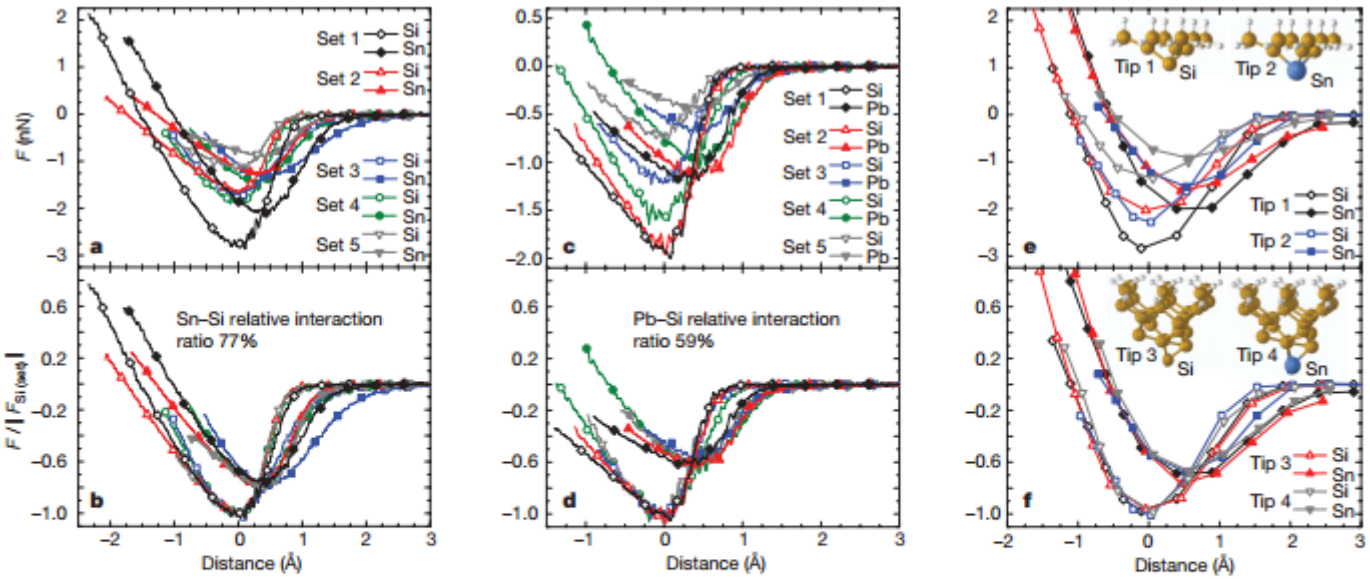

Figure 2 | Probing short-range chemical interaction forces. **a**, Sets of short-range force curves obtained over structurally equivalent Sn and Si atoms. All curves are obtained using identical acquisition and analysis protocols, but the tips differ from set to set. **b**, The same force curves as in **a**, but the curves in each set are now normalized to the absolute value of the minimum short-range force of the Si curve ($|F_{Si(set)}|$). **c**, **d**, Sets of short-range force curves for Pb and Si, obtained in the same way as for Sn and Si, before (**c**) and after (**d**) normalization. The average relative interaction ratios calibrated against Si, or the maximum attractive short-range forces for Sn and Pb relative to those of Si (77% and 59%, respectively), provide an intrinsic signature for the chemical identification of individual atoms. Each experimental force characteristic shown here was obtained from the measurement of a hundred spectroscopic curves (see Methods for details). The acquisition parameters are available in the Supplementary Information. **e**, **f**, Chemical force curves calculated for different tip-apex models (see insets for structural and chemical characteristics) over the Sn and Si atoms of the $(\sqrt{3} \times \sqrt{3})$ R30° surface model shown in Fig. 1b. The curves are shown before (**e**) and after (**f**) normalization. In both the experimental and the calculated short-range force curves, the distance axes denote the tip–sample relative displacement (see Methods for details).

Seizo Morita & Óscar custance, Osaka university, Jap

Chemical identification of individual surface atoms

The images were acquired close to the onset of the short-range interaction

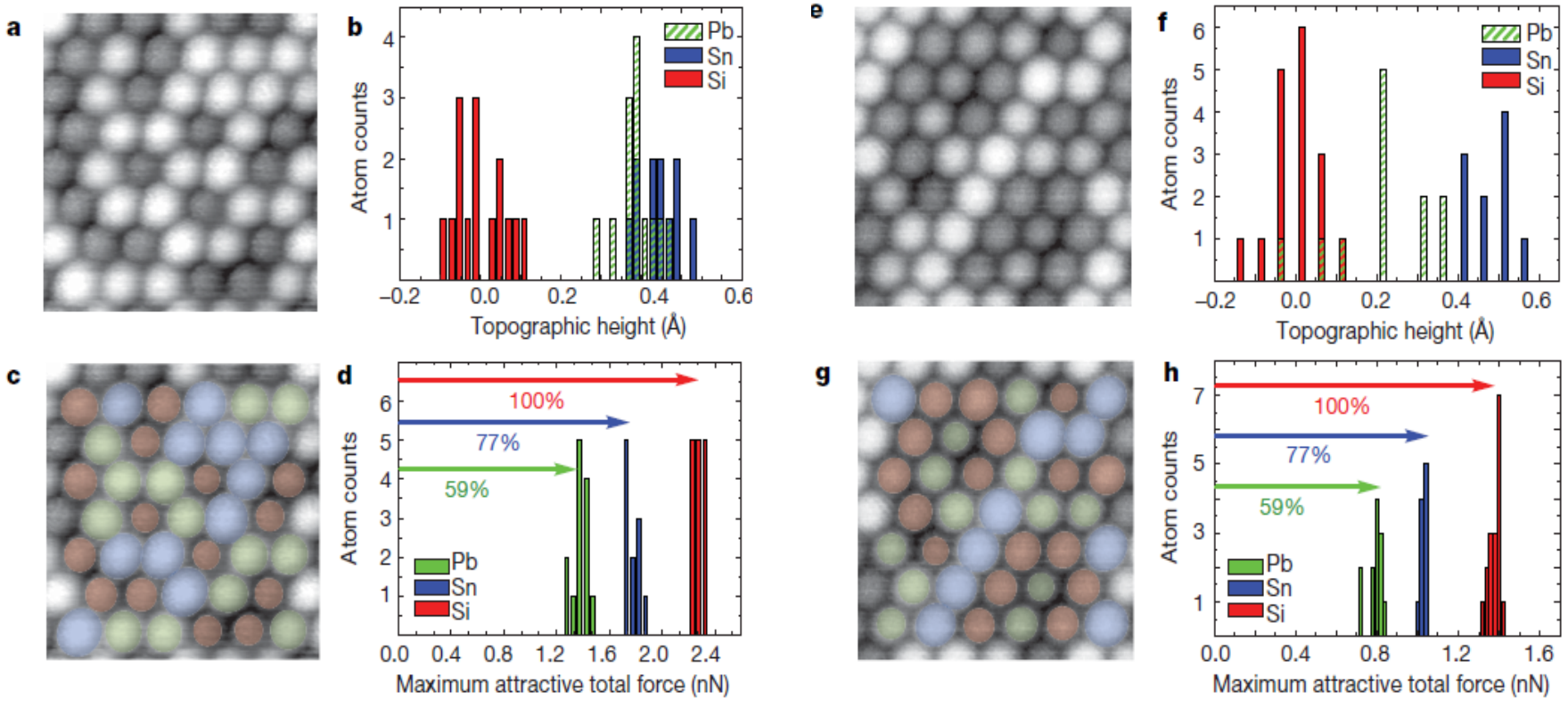

b: Pb and Sn atoms with few nearest-neighboring Si atoms appear indistinguishable in topography
f: Pb atoms are almost completely surrounded by Si atoms are indistinguishable from the surrounding Si atoms

Nature 446, 64 (2007)

Gerhaed Meyer, IBM research- Zuri

Measuring the charge state of an adatom

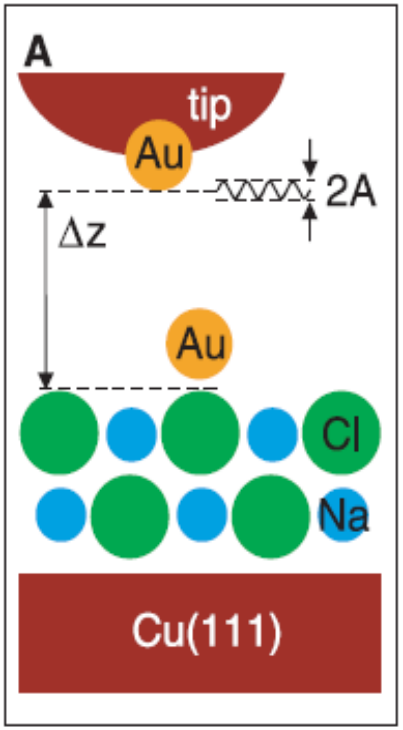

Q plus
5 K
A=0.2 Å

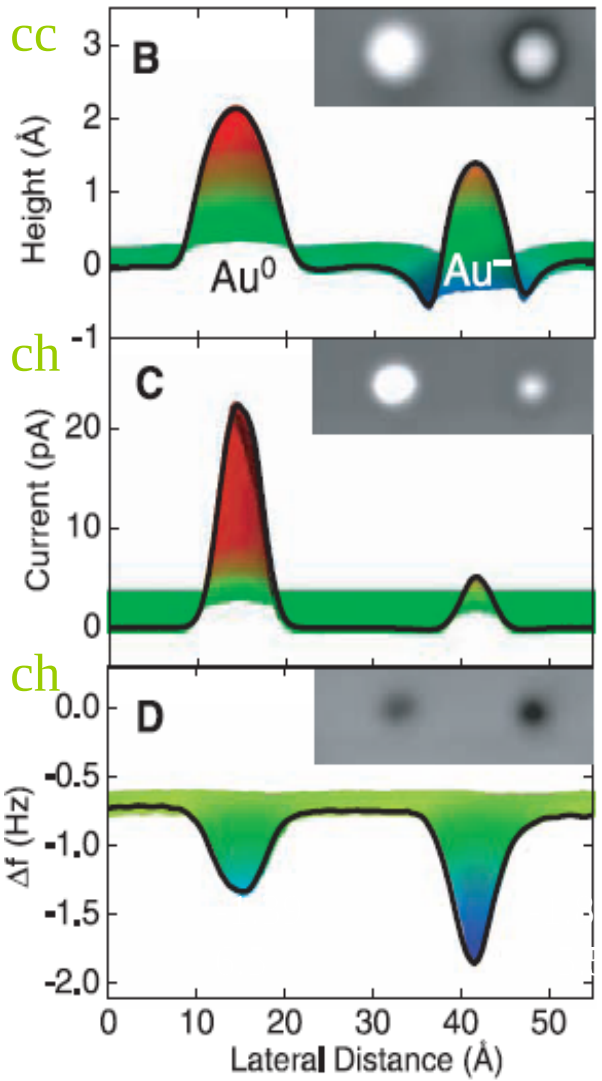

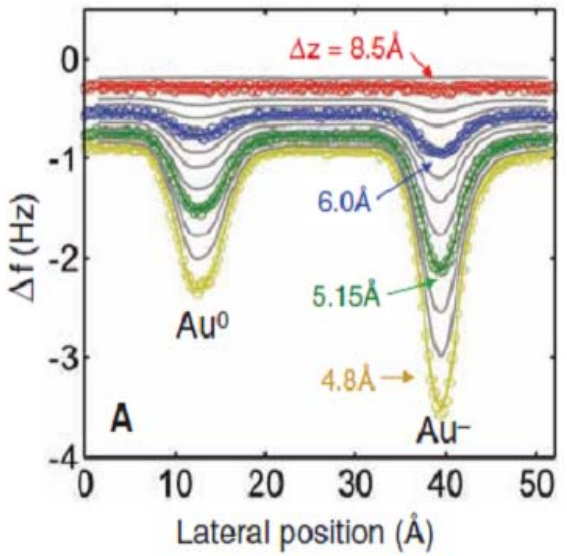

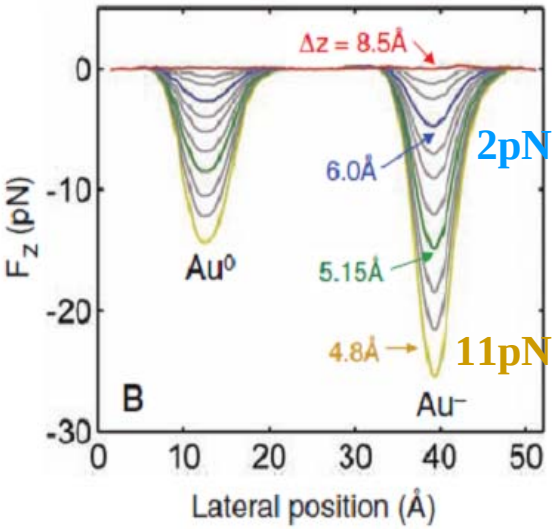

Science 324, 1428 (2009)

Measuring the charge state of an adatom

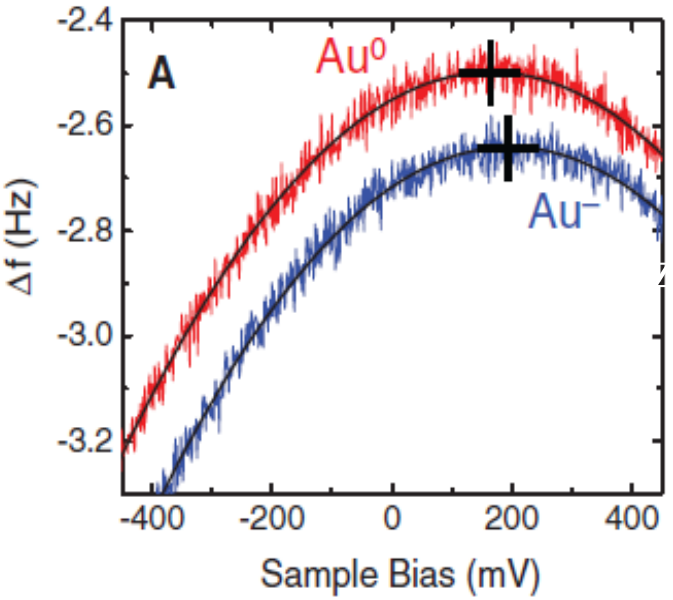

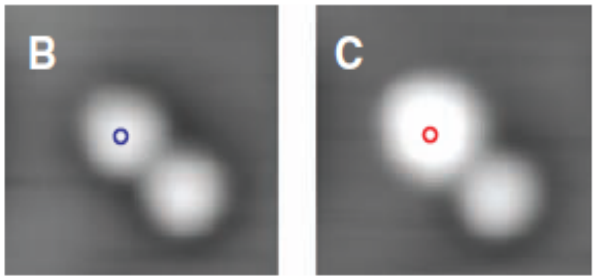

measure Δ f (V) above Au−
apply a bias voltage pulse (–1 V) to switch the charge state
measure Δ f (V) once more
STM images were taken before and after this routine

Local contact potential difference

$LCPD=eV_{CPD}$

工欲善其事，必先利其器。

孔子. 论语· 魏灵公